Limnology and Oceanography
January 2021, Volume 66, Issue 1, Pages 141-157
https://doi.org/10.1002/lno.11593
https://archimer.ifremer.fr/doc/00652/76419/

Trophic ecology of a blooming jellyfish (*Aurelia coerulea*) in a Mediterranean coastal lagoon

Marques Raquel [1, *] , Bonnet Delphine [1], Carré Claire [2], Roques Cécile [3], Darnaude Audrey M. [3]

[1] MARBEC Univ. Montpellier, CNRS, Ifremer, IRD Montpellier , France

* Corresponding author : Raquel Marques, email address : marques.rfs@gmail.com

Abstract :

The current lack of knowledge on the trophic ecology of scyphozoans, particularly at the benthic stage, prevents a full understanding of the controls on many jellyfish blooms. The blooming scyphozoan (Aurelia coerulea) completes its entire life cycle in the Thau lagoon (southern France), where the annual population dynamics of both its benthic and pelagic stages have been described. This offered an exceptional framework to investigate the trophic processes regulating jellyfish populations over time. To this aim, stable isotopic signature analysis (δ13C and δ15N) was used to infer the diet of both A. coerulea scyphistomae and medusae over 1 year. These results were matched with medusae gut content analysis and with the monthly abundances of local plankton groups. Lastly, the isotopic signatures of A. coerulea scyphistomae and medusae were compared with those of the oysters (Crassostrea gigas) cultivated in the lagoon to evaluate the potential interspecific trophic competition. The results revealed two seasonal shifts in the trophic niche of A. coerulea and substantial overlap between the diets of its benthic and pelagic stages. Conversely, trophic niche overlaps with the oysters were restricted, suggesting a limited impact of the local jellyfish bloom on shellfish production. Phytoplankton, microzooplankton, mesozooplankton, and sedimentary organic matter were all important food sources during critical periods of A. coerulea life-cycle. However, microzooplankton abundance was found to be key for the production of buds by the scyphistomae and, therefore it is likely to control the benthic population size and, thereby, to modulate the intensity of its annual bloom in Thau.

Introduction

Due to the impact of their conspicuous blooms on coastal ecosystems functioning and economic activities, jellyfish have received increasing scientific attention during the last decades (Purcell 2012). In particular, the ecological drivers of jellyfish mass occurrences have been investigated, revealing a complex interaction of natural (e.g. Condon et al. 2012) and anthropogenic (e.g. Purcell 2012) causes. However, uncovering the drivers of blooms is particularly challenging for most scyphozoan blooming species because their life-cycle comprises a benthic (scyphistomae) and a pelagic (ephyrae and medusae) phase (e.g. Lucas 2001). Therefore, bloom formation is a joint consequence of the production of pelagic ephyrae by the benthic scyphistomae and of their survival and growth into medusae. As a result, the ecology of both life stages controls bloom intensity.

Bottom-up processes within food webs often play a key role in ecological systems functioning and are amongst the most important drivers of jellyfish blooms (Boero et al. 2008). Food quality and availability are known to control the production of ephyrae by the scyphistomae (Han and Uye 2010; Ikeda et al. 2017) and to modulate the growth rate of medusae (Ishii and Båmstedt 1998). This supports the need for comprehensive studies on the trophic ecology of both life stages in the field. Yet, although information is growing on the trophic ecology of medusae (e.g. Javidpour et al. 2016; Milisenda et al. 2018), the diet of jellyfish scyphistomae is still poorly known.

Jellyfish from the *Aurelia* genus are present globally in coastal areas and are among the most common scyphozoans that form blooms (Mills 2001). Large accumulations of *Aurelia* spp. have been reported all around the world, including in the Mediterranean, where they occur mainly in protected waters and semi-enclosed seas (Mills 2001). Their medusae have been described as zooplanktivorous, with a dominance of mesozooplankton, especially copepods, in their diet (e.g. Ishii and Tanaka 2001; Lo and Chen 2008). However, while

65 microzooplankton and benthic food sources have been considered for long as negligible food
66 sources for jellyfish, recent findings based on new techniques (such as stable isotope analysis)
67 suggest the opposite (Javidpour et al. 2016). In laboratory studies, newly hatched *Artemia* sp.
68 are usually provided as food (e.g. Han and Uye 2010, Hubot et al. 2017), but the few studies
69 regarding the diet of *Aurelia* sp. scyphistomae in the wild suggest that they eat a mix of
70 phytoplankton (Huang et al. 2015), microzooplankton (Kamiyama 2013) and small
71 mesozooplankton species (e.g. copepods, cladocerans, gelatinous zooplankton; Östman 1997).
72 Considering the critical role of scyphistomae in the formation of scyphozoans blooms, it is
73 urgent to specify natural prey preferences in *Aurelia* species and the potential trophic
74 competition among their benthic and pelagic stages to understand blooms formation in this
75 genus and evaluate their ecological consequences.
76 Situated along the North-western Mediterranean coast, the Thau lagoon offered an
77 exceptional framework for this. Indeed, this lagoon presents the rare particularity to harbour a
78 complete resident population of *Aurelia coerulea* (Bonnet et al. 2012; Marques et al. 2015a),
79 which allows investigating the trophic processes that regulate its population dynamics at both
80 stages. The scyphistomae of *A. coerulea* are widespread in the lagoon, fixed mainly on
81 biofouling organisms that grow on anthropogenic structures (predominantly on oysters and
82 mussels; Marques et al. 2015a). They are present all year round, with a peak of coverage in
83 the Spring (April) and lower densities in the Summer and Autumn (Marques et al. 2019).
84 Ephyrae appear in the early winter (November – December) and give rise to adult medusae at
85 the beginning of the Spring (April – May), generating the annual jellyfish bloom, which
86 persists until June – July (Bonnet et al. 2012; Marques et al. 2015b). Because no clear link
87 was found between the abundance of mesozooplankton in the lagoon and the benthic
88 population dynamics of *A. coerulea*, it was suggested that other food sources might sustain

the species local production (Marques et al. 2019). Nevertheless, further confirmation is still required in this regard.

Coastal lagoons are usually very productive environments, where high continental inputs in nutrients and particulate organic matter sustain high and diversified primary and secondary productions (Nixon et al. 1995). This benefits the whole food web and enhances the growth of lagoon predators like juvenile fish (Escalas et al. 2015). In Thau, it also supports a massive shellfish production: ~10% of the Pacific oysters *Crassostrea gigas* produced in France come from the lagoon, with a yearly shellfish production of 15 000 tons (Mongruel et al. 2013).

In this context, the present work not only aimed to describe the trophic ecology of both the benthic and the pelagic life-stages of *A. coerulea* in Thau and assess its influence on critical periods of population dynamics of this jellyfish (e.g. peak of bud production, strobilation, and medusae growth), but also to evaluate whether *A. coerulea* medusae and scyphistomae compete for food with the Pacific oysters reared in the lagoon. For this, we combined medusae gut content assessments with stable isotopes analysis. This latter technique has been increasingly used to study the structure and transfer of organic matter within coastal food webs (Layman et al. 2012) and has recently allowed uncovering the diet, trophic levels, and trophic interactions of different jellyfish species (Fleming et al. 2015; Javidpour et al. 2016; Milisenda et al. 2018). Using it to explore the changes in *A. coerulea* diet during a full annual cycle should allow assessing whether its benthic and pelagic stages occupy the same trophic niche than the oysters cultivated in the lagoon. This strongly contributes to a better understanding of the impacts of *A. coerulea* blooms on the local shellfish production.

Material and Methods

Study site

The Thau lagoon is a semi-enclosed marine coastal lagoon of 75 km^2 area, connected to the Mediterranean Sea by three narrow channels (Fig. 1). It is relatively shallow, with mean and maximum depths of 4 and 10 m, respectively (except for a localized depression of 24 m). The local tidal range (< 1m) is weak, so water residence time in the lagoon is globally high (1–-4 months) and strongly influenced by seasonal strong wind events (Millet and Cecchi 1992). The lagoon environment parameters show strong seasonal variations, characteristic of temperate regions, with temperature and salinity at their lowest in the winter (with minimum values of 7.6 and 35.0, respectively) and at their highest in the summer (with maximum values of 25.8 ºC and 39.6, respectively; Marques et al 2019). The lagoon mainly receives water from the Sète canal that connects it to the Mediterranean Sea and from several small intermittent rivers that drain its catchment area (290 km^2, Plus et al. 2006). These later dry out between May and September and show occasional flash floods in the wet season (Fouilland et al. 2012). As a result, marine conditions prevail in the lagoon, the annual influence of the freshwater coming from the watershed being highly dependent on the intensity of rainfall events during the winter (Plus et al. 2006). With regards to anthropogenic influence, the lagoon is under multiple pressures due to the presence of the touristic city of Sète and many small villages and agriculture fields on its coastline. Shellfish farming is the most important economic activity on the lagoon (Mongruel et al. 2013): around 20% of its surface is occupied by farms, mainly in the northern and north-western parts (Fig. 1).

Sampling

For this study, the jellyfish and their potential food sources were sampled in the eastern part of the lagoon, at two close sites where the benthic and the pelagic population dynamics of *A. coerulea* had been previously described (Bonnet et al. 2012; Marques et al. 2015b; Marques et al. 2019). Both sites (benthic sampling site: 43°25'31.1"N; 03°42'0.9"E

and pelagic sampling site: 43º23’59.1’’N; 03º36’37.2’’E; Fig. 1) are located on soft-bottom sediments punctuated by sparse seagrass meadows and are strongly influenced by marine water influxes due to their proximity to the Sète channel, which connects the lagoon to the Mediterranean Sea.

A. coerulea scyphistomae were collected monthly on a partially submerged boat present at the benthic sampling site (see Marques et al. 2019 for more details), over an entire calendar year (from January 2017 to January 2018). For this, mussel shells with sizeable aggregates of scyphistomae attached on their underside surface (three per sampling date) were collected directly on the surface of the boat by SCUBA diving. They were brought to the laboratory in ambient water and placed in 0.2-µm-filtered seawater (ca. 20ºC) for about 2h to ensure all scyphistomae had empty guts. Fifty individual scyphistomae were then collected under a dissecting microscope (Olympus SZ40; Olympus KL 1500 LCD), using needles and tweezers to carefully detach them, and preserved in cryotubes at –30ºC.

The pelagic ephyrae of *A. coerulea* are usually present in the lagoon from November to April (Bonnet et al. 2012; Marques et al. 2015b). However, because stable isotope analysis requires pooling high numbers of these small organisms to be applicable, sampling for this life stage in this work was successful in January 2018 only. The ephyrae were collected near the water surface at the pelagic sampling site, by horizontal towing, using a modified WP2 plankton net (1.2 m long, 50-cm opening, and 200-µm mesh). In the laboratory, they were picked and kept for ca. 2h in filtered seawater to allow for complete gut evacuation. Then 50 individuals were pooled per sample and preserved at –30ºC.

A. coerulea medusae (i.e., pelagic individuals with bell diameter > 1 cm), were collected every two weeks at the pelagic sampling site, from March to June 2017, i.e., over the entire period of their presence in the lagoon. They were collected in surface waters using hand nets and transported to the laboratory in ambient water. Five individual medusae were then

randomly selected and prepared for stomach content analysis. For this, they were each partially dried on a paper towel to remove excess water, measured (bell diameter in cm), weighted (total wet weight in g), and individually preserved in 4% buffered formaldehyde. The remaining medusae were kept for ca. 2h in 0.2 µm filtered seawater (ca. 20ºC) to empty their guts. Three of them were then placed on a paper towel for about 1 minute (30 s on each side) to remove excess water, weighed, and measured. As bell tissue is the most suitable body part for stable isotope analysis in jellyfish (D'Ambra et al. 2014), gonads, oral arms, and gastric pouches were removed from each medusa. The remaining individual bell tissues were preserved separately at -30ºC. In March 2017, due to the small size of the medusae (ca. 2 cm bell diameter), eight complete individuals were pooled per replicate before preservation at -30ºC.

For this work both the plankton and the sedimentary organic matter of the lagoon were also sampled as they both constitute potential food sources for *A. coerulea*. Samples for these two components were collected at pelagic and benthic sampling sites, respectively, on the same sampling dates as *A. coerulea* medusae and scyphistomae collection. Within the plankton, the fraction larger than 200 µm, that between 60 and 200 µm and that between 20 and 60 µm were assumed to be composed mainly by mesozooplankton, microzooplankton, and phytoplankton, respectively. Mesozooplankton samples were collected near the surface, by horizontal towing, using a modified WP2 plankton net (length: 1.2 m; opening area: 50 cm; mesh size: 200 µm). Once in the laboratory, each sample was filtered through a 60 µm mesh sieve to eliminate excess water and divided into five subsamples. Microzooplankton and phytoplankton samples were also collected by horizontal towing near the surface, but using a phytoplankton net (length: 1 m; opening area: 30 cm; mesh size: 20 µm). Once in the laboratory, each sample was filtered through a 200-µm sieve. The size fraction > 200 µm was discarded. The remaining sample was then separated into the two size fractions,

corresponding to microzooplankton and phytoplankton, using a 60 µm sieve, and then divided into 5 subsamples. For each plankton size fraction, the subsamples were collected separately on pre-combusted (500ºC for 24h) Whatman GF/F filters. Two filters of each plankton component were acidified with 1% HCl and triple rinsed with distilled water to remove inorganic carbon, which can bias C stable isotope results (Yokoyama et al. 2005). The remaining non-acidified filters were used for N stable isotope analysis, since sample acidification may affect the stable isotope signature for this element (Pinnegar and Polunin 1999). All samples were preserved at –30ºC until further analysis. For sedimentary organic matter, the first 2 cm of the sediment were collected by SCUBA diving at the benthic monitoring site. Samples (2 replicates) were carefully scrutinized to eliminate any large organisms, sediment inorganic particles, or vegetal debris, before preservation at –30ºC.

To investigate the trophic interactions between *A. coerulea* and the local oysters, both wild and cultivated individuals of *Crassostrea gigas* were sampled seasonally from October 2017 to August 2018, including during the peak of the jellyfish bloom (which occurred in June in 2018). Wild oysters (mean size: 11.5 ± 2.0 cm) were collected by SCUBA diving at the benthic monitoring site, while the cultivated ones (mean size: 11.9 ± 1.0 cm) were obtained from the shellfish producer *Huitres-Bouzigues.com*. Immediately after their removal from the lagoon, the oysters were transported to the laboratory in ambient water, measured and carefully dissected to collect their adductor muscle. The muscle tissues were then rinsed with distilled water and preserved separately at –30ºC until further analysis.

In situ abundance of plankton in the Thau lagoon

Phytoplankton, microzooplankton and mesozooplankton samples were collected at the pelagic monitoring site, every two weeks from January to June 2017 and monthly onwards, until December 2017. For phytoplankton, 10 to 20L of surface water were collected, filtered with a

15-µm-mesh net, and preserved with 2% buffered formaldehyde. For microzooplankton, a subsample of 30 ml of surface water was preserved with 2% buffered formaldehyde (to estimate ciliates' abundance) and one of 110 ml was preserved with Lugol's solution (to estimate heterotrophic flagellates' abundance). Phytoplankton and microzooplankton species were identified and counted using sedimentation chambers and an inverted microscope (Olympus IX70) following the Utermöhl method (Utermöhl 1958). Mesozooplankton samples were collected near the surface by horizontal towing using a modified WP2 plankton net (1.2 m long, 50-cm opening, and 200-µm mesh). Samples were immediately preserved in 4% buffered formaldehyde until further analysis in the laboratory. Mesozooplankton abundance was determined by counting organisms under a dissecting microscope (Olympus SZX7 – ILLT). The diversity of mesozooplankton was not assessed.

Gut content analyses

To evaluate the diet of *A. coerulea* medusae, their gastric pouches, oral arms, and the preserving solution were examined under a dissecting microscope (Olympus SZX7 – ILLT). Although *A. coerulea* medusae were present in the lagoon from March, most individuals exhibited empty guts during this month. Therefore, gut content analysis was only performed on the medusae collected between April and June. For this, only complete exoskeletons were considered for prey identification. This was done to the lowest possible taxonomic level, although the level of exoskeleton digestion often precluded prey identification down to the species level. The importance of each prey in the diet was expressed by the following indices: (i) the frequency of occurrence (in %), which represents the percentage of medusae with the prey *i* in their guts among all those that had non-empty guts; (ii) the index of relative importance (in %), representing the percentage of prey *i* in relation to the total number of prey

items found in the non-empty guts; and (iii) the mean abundance of prey *i* in non-empty guts (in ind. medusae^{-1}).

Stable isotope analysis

All filters containing plankton (phytoplankton, microzooplankton, and mesozooplankton) were oven-dried at 60ºC for 48h and the biological material was gently scraped off the filter surface. Samples for the sedimentary organic matter, the oysters, *A. coerulea* medusae, scyphistomae, and ephyrae were freeze-dried for 48h and ground to a fine powder using a mortar and pestle. The sedimentary organic matter samples were divided into two subsamples. One half was used directly for N stable isotope analysis. The remaining subsample was acidified with 1% HCl to remove carbonates before C stable isotope analysis, rinsed several times with distilled water, and oven-dried at 70ºC.

Stable isotopic analyses for biological samples were performed using a PDZ Europa ANCA-GSL elemental analyser interfaced with a PDZ Europa 20-20 isotope ratio mass spectrometer (Sercon Ltd., Cheshire, UK). Measurements of $\delta^{13}C$ and $\delta^{15}N$ signatures were performed each on 1.5 to 4 mg of dry samples, with exception of the medusae, for which ca. 10 mg of dry sample was required for successful analysis, after salt content correction, based on dry weight and ash-free dry weight relationships (Lucas et al. 1994; Pitt et al. 2009). Sedimentary organic matter samples (of ca. 55 mg each) were analysed using an Elementar Vario EL Cube or Micro Cube elemental analyser (Elementar Analysensysteme GmbH, Hanau, Germany) interfaced to a PDZ Europa 20-20 isotope ratio mass spectrometer (Sercon Ltd., Cheshire, UK). Calibration was performed against NIST Standard Reference Materials (IAEA-600, USGS-40, USGS-41, USGS-42, USGS-43, USGS-61, USGS-64, and USGS-65). Isotope ratios of all samples were expressed as parts per thousand (‰) differences from the internal

reference standards (glutamic acid, alfalfa flour, nylon 6, bovine liver, and enriched alanine) using the following equation:

$$\delta X = \left[\left(\frac{R_{sample}}{R_{standard}}\right) - 1\right] \times 1000$$

where *X* is the ^{13}C or ^{15}N and R is the corresponding ratio, $^{13}C/^{12}C$ or $^{15}N/^{14}N$.

As the lipid content of organisms affects their $\delta^{13}C$ signatures, $\delta^{13}C$ correction is required when C:N is higher than 3.5 (Post et al. 2007). Therefore, the $\delta^{13}C$ values obtained for *A. coerulea* scyphistomae and medusae (mean C:N 3.7 ± 0.1 and 3.9 ± 0.6, respectively) and for the mesozooplankton (mean C:N of 6.9 ± 3.0) were corrected ($\delta^{13}C_{corr}$) according to the equations proposed by D'Ambra et al. (2014) for jellyfish:

$$\delta^{13}C_{corr} = \delta^{13}C_{initial} - 9.43 + 2.69 \times C{:}N$$

and by Syväranta and Rautio (2010) for zooplankton:

$$\delta^{13}C_{corr} = \delta^{13}C_{initial} + 7.95 \times \left(\frac{C{:}N - 3.8}{C{:}N}\right)$$

Relationship between benthic population dynamics and plankton abundance

Data on *A. coerulea* benthic population dynamics were obtained from Marques et al. (2019). Generalized linear models (using linear and logistic regressions, without interactions) were employed to assess the respective contributions of the absolute abundances of the non-averaged phytoplankton, the microzooplankton and the mesozooplankton (after logarithmic transformation ln (x+1)) to temporal trends in the scyphistomae density (% coverage) and in the proportion of the scyphistomae producing buds. The models were validated by examination of residuals versus fitted values plots (Zuur et al. 2009).

Determination of Isotopic Niche Periods

To reveal potential shifts in the trophic niches of *A. coerulea* scyphistomae and medusae during the year and identify the periods when they present unchanging isotopic signatures (hereafter "Isotopic Niche Periods"), a cluster analysis was performed on the monthly mean isotopic values of both life stages (Jain 2010). For this, partitioning algorithms, based on the k-means clustering method, were applied using the package “factoextra” (Kassambara and Mundt 2017). The k-means approach subdivides the data into a set of k groups so that the sum of squares from the data points to the center of each group is minimized (Kassambara and Mundt 2017). This clustering approach allowed to identify the successive isotopic niche periods for both life stages, providing the basis for identifying their successive sources of organic matter during the year.

Assessment of potential intra- and interspecific trophic competition

Our sampling design allowed for reliable estimation of the potential intraspecific trophic competition between *A. coerulea* scyphistomae and medusae within each isotopic niche period. However, because oyster and jellyfish samples were collected in different years (except for one isotopic niche period), the trophic competition between the two species was only investigated globally, assuming that interannual variability in the trophic niche in the two species is negligible. In both cases, the Bayesian framework proposed by Jackson et al. (2011) for evaluating trophic competition was used. For this, Bayesian multivariate normal distributions were first fitted to the isotopic signatures of all organisms. Then, the overlap between their trophic niches was calculated based on maximum likelihood fitted ellipses, using the function “maxLikOverlap” from the R package “SIBER” (Jackson et al. 2011).

Determination of jellyfish diet using Stable isotope analysis

Differences in isotopic signatures ($\delta^{13}C$ and $\delta^{15}N$) among the main local potential food sources (phytoplankton, microzooplankton, mesozooplankton, and sedimentary organic matter) were tested by a PERMANOVA (Anderson 2017) on the log10 transformed Bray-Curtis distance matrix (– $\delta^{13}C$ and $\delta^{15}N$), made using the package "vegan" (Oksanen et al. 2019), followed by pairwise comparisons made using the "pairwiseAdonis" package in R (Martinez Arbizu 2019). Sources with no significant differences were grouped for subsequent analyses.

Diet compositions for *A. coerulea* scyphistomae and medusae within each isotopic niche period were assessed using Bayesian mixing models developed specifically for stable isotope analysis ("MixSIAR" package, Stock and Semmens 2016). By generating the probability distributions of all potential mixing solutions with the associated confidence intervals (based on 300 000 chain length), this approach allows identifying the most likely contribution for each food source. MixSIAR further provides a graphical user interface that allows investigation of the contributions of multiple food sources to the diet of target predators, considering not only the isotopic signatures ($\delta^{13}C$ and $\delta^{15}N$) of the sources and the predators but also the uncertainties and variability around these estimates. Finally, the method allows us to use different isotopic fractionation factors at each trophic level. As previously performed in other studies on jellyfish diet (e.g. Morais et al. 2017), the fractionation values applied here for both *A. coerulea* life stages were those proposed by Vander Zanden and Rasmussen (2001): for $\delta^{13}C$ we used 0.47 ± 1.23 ‰ in all cases, while for $\delta^{15}N$ we used 2.52 ± 2.5 ‰ and 3.23 ± 0.41 ‰ according to the type of food consumed (plant vs. animal, respectively). Like Fleming et al. (2015) and Milisenda et al. (2018), we did not use the fractionation values reported by D'Ambra et al. (2014), since they are very distinct from those mostly used in the literature (Vander Zanden and Rasmussen 2001; Post 2002) and they still require further laboratory corroboration (D'Ambra et al. 2014).

The basal tissue turnover rate for *Aurelia* sp. is of ca. 1 ‰ day^{-1} for $\delta^{13}C$ and 2‰ day^{-1} for $\delta^{15}N$, and it takes 18 to 20 days for the tissues of this jellyfish to reach the stable isotopic equilibrium with the food ingested (D'Ambra et al. 2014). To account for such turnover rates, MixSIAR models were run by isotopic niche period, but jellyfish signatures at a given sampling date were matched with those recorded one month earlier for all potential food sources.

Results

Medusae gut contents

Among the 25 medusae collected for gut content analysis from April to June 2017, 21 had food in their guts. The bell diameter of these individuals did not vary significantly over time (ANOVA, $F_2 = 1.4$, p-value = 0.2), remaining at ca. 8.5 cm. Overall, gut content composition predominantly consisted of mesozooplankton (>88%). Microzooplankton (mainly tintinnids) and phytoplankton (mainly diatoms and dinoflagellates) represented only 8 and 4% of the total prey identified, respectively, and they were only found in the guts in April and May (Fig. 2, Table 1, Supplementary Table 1). In April, phytoplankton and microzooplankton occurred in 20 and 60% of the guts analysed, but their relative importance and abundances were still low (< 7.5% and < 2.2 $ind.medusa^{-1}$, respectively, Table 1). In May, frequency of occurrence increased for phytoplankton (33%) and slightly decreased for microzooplankton (56%) and showed a growing trend of their relative importance for both groups (5.6 and 12.5%, respectively, Fig. 2). Indeed, in May, microzooplankton relative importance was higher than some mesozooplankton organisms, like the "other crustaceans" group, which includes cladocerans and ostracods (10.0%; Table 1, Supplementary Table 1). Masses of unidentified organic matter were also recurrently observed over the entire study period.

Twenty-four different taxa of mesozooplankton were identified in the guts of the medusae, but, among them, copepods and nauplii (from cirripeds and copepods) dominated. They occurred in 40 to 88.9% of the guts analysed and represented up to 46.3% of the prey identified (in June, Table 1). The maximum average abundance of mesozooplankton organisms in the guts (26.2 ± 35.4 ind.medusae^{-1}) was recorded in April when non-crustacean taxa (mainly gastropod veliger), and copepods represented more than 80% of the prey identified in medusae gut contents (Table 1). Nauplii (index of relative importance = 31.3%) were the most important mesozooplanktonic prey in the guts in May, while in June, copepods dominated (index of relative importance = 46.3%, Table1).

Prey availability and relationship with benthic population dynamics

Prey abundances in *A. coerulea* medusae gut contents did not reflect their availability in the water column. The abundances of phytoplankton, microzooplankton, and mesozooplankton in the lagoon all showed high intra-annual variability (Fig. 3), with respective peaks in January (25 138 ± 34 047 cell.L^{-1}) and May (35 794 ± 18 374 and cell.L^{-1}), in February, April, and September (> 6 200 cell.L^{-1}) and in June (90 895 ± 107 072 ind.m^{-3}). Thus, when *A. coerulea* medusae were present in the water column, the planktonic community was mainly dominated by phytoplankton in April and May, and by mesozooplankton in March and June, while the microzooplankton showed consistently lower abundances despite a small peak in April. In terms of species composition, the most abundant phytoplanktonic and microzooplanktonic taxa in the water column during the study period were *Chaetoceros* sp. and *Strombidium* sp., respectively (Supplementary Table 2). Mesozooplankton diversity was not assessed, but *Acartia* sp. are recurrently the most abundant taxa in Thau (Boyer et al. 2013).

Annual variations in scyphistomae coverage, which peaked in April (11.6 ± 3.7 %, Marques et al. 2019), were positively correlated with the non-averaged abundance of phytoplankton

(Generalized linear models, t-value = 2.97, p-value = 0.01, Table 2, Fig. 4). In turn, fluctuations in the mean percentage of scyphistomae producing buds, which varied between 0.4 ± 0.7 % in November and 25.2 ± 7.3 % in September (Marques et al. 2019, Fig. 4), were positively correlated with variations in non-averaged microzooplankton abundance (Generalized linear models, t-value = 10.19, p-value < 0.01, Table 2).

Temporal variation of A. coerulea isotopic signatures

$\delta^{13}C$ and $\delta^{15}N$ signatures showed significant temporal variation for both the scyphistomae and medusae (one-way PERMANOVA, Pseudo-F_{11} = 22.7, p-value < 0.01 and Pseudo-F_3 = 38.6, p-value = 0.001, respectively), but differences between life stages were never significant during the period of medusae presence, from March to June (one-way PERMANOVA, Pseudo-F_1 = 1, p-value = 0.4). The mean bell diameter of the medusae used for stable isotope analysis, showed a sharp increase between March (1.0 ± 0.3 cm) and June (8.9 ± 1.1 cm), with an estimated overall growth of 0.8 $mm.day^{-1}$. Over this period, medusae $\delta^{13}C$ signatures increased progressively from –23.4 ± 0.1‰ to –19.4 ± 0.5‰, while their $\delta^{15}N$ signatures remained stable for the first three months (at ca. 8.1‰), and increased (to a maximum at 8.9 ± 0.3‰) only in June (Fig. 5). For the scyphistomae, minimum $\delta^{13}C$ values were registered at the beginning of the study period (in January 2017, mean: –23.4 ± 0.1‰). The $\delta^{13}C$ signatures then increased to reach maximum values in June, July, and August (> –19.4‰) before decreasing again until January 2018 (–22.3 ± 0.4‰). The $\delta^{15}N$ signatures of scyphistomae showed a similar temporal trend, with low values at the beginning and the end of the study period (8.3 ± 0.1‰ and 8.0 ± 0.4‰ in January 2017 and 2018, respectively), and maximum values in July and August (>9‰). The minimum values of $\delta^{15}N$ signatures, though, were observed in February 2017 (7.1 ± 0.5‰). The average $\delta^{13}C$ and $\delta^{15}N$ signatures of the ephyrae collected in January 2018 (bell diameter of 0.21 ± 0.1 cm) were of –22.8 ± 0.1‰ and 8.5 ±

0.3‰, respectively. They did not differ significantly from those of the scyphistomae collected at the same sampling time (T-test, t = –1.9, df = 2.3 p-value = 0.2 and t =1.2, df = 2.6, p-value = 0.3, for $\delta^{13}C$ and $\delta^{15}N$ respectively).

The clustering analysis revealed three distinct groups of isotopic signatures among the monthly values obtained for all life stages of *A. coerulea* (Fig. 6) allowing to identify three isotopic niche periods during the year.: Period 1 gathered the $\delta^{13}C$ and $\delta^{15}N$ signatures of all life stages from December to April, irrespective of the year (2017 or 2018). Period 2 reflected the signatures of both the medusae and the scyphistomae from June to August. Period 3 corresponded to the signatures of the scyphistomae from September to November, together with the signatures of the medusae and the scyphistomae in May. However, May showed a particular sharp shift in $\delta^{13}C$ and $\delta^{15}N$ reflecting the rapid transition from the isotopic signature of period 1 to that of period 2 and, therefore, it was not included in any isotopic niche period.

Monthly variability of organic matter sources signatures

$\delta^{13}C$ and $\delta^{15}N$ signatures varied significantly according to the organic matter source and the month (significant interaction, PERMANOVA, *Pseudo-*F_{17} = 23.1, p-value < 0.01; Fig. 7). For carbon signatures, minimum $\delta^{13}C$ values for phytoplankton, microzooplankton and mesozooplankton (of –24.7 ± 0.3, –23.3 ± 0.1 and –23.7 ± 0.0 ‰, respectively) were all observed in March. A sharp increase in $\delta^{13}C$ was observed in the following months, with maximums in May for mesozooplankton (–18.8 ± 0.2 ‰) and in November for phytoplankton (–19.0 ± 0.0 ‰) and microzooplankton (19.9 ± 0.1 ‰). Concerning nitrogen signatures, mesozooplankton was the organic matter source with the highest $\delta^{15}N$ values, ranging from 7.3 ± 0.3 (in May) to 8.4 ± 0.0‰ (in March). Minimum $\delta^{15}N$ values were also observed in May for the phytoplankton and the microzooplankton (at 5.8 ± 0.5 ‰ and 6.0 ± 0.3 ‰,

433 respectively) but, for these two organic matter sources, maximum values were observed in
434 July (at 6.7 ± 0.3 ‰ and 7.4 ± 0.2 ‰, respectively). Moreover, another peak in $\delta^{15}N$ (at 6.7 ±
435 0.0 ‰) was observed in February for the phytoplankton. For the sedimentary organic matter,
436 both the $\delta^{13}C$ and $\delta^{15}N$ signatures decreased from March (–18.9‰ and 5.8‰, respectively) to
437 April (–20.7‰ and 5.5‰, respectively), remaining constant afterwards.
438
439 *Contribution of organic matter sources to A. coerulea isotopic signatures*
440 Since the $\delta^{13}C$ and $\delta^{15}N$ signatures of the phytoplankton and the microzooplankton were not
441 significantly different (PERMANOVA post-hoc test, Pseudo-F_1 = 5.7, adjusted p-value =
442 0.17) these two organic matter sources were pooled as Small Plankton group in the mixing
443 models used to assess the diet of *A. coerulea*. The remaining sources were included
444 individually in the models (Table 3). The contribution of each source was found to vary
445 according to the isotopic niche periods and the life stage of *A. coerulea* considered (Fig. 8).
446 For the scyphistomae, the model suggested a dietary shift from small plankton consumption in
447 period 1 (93.3%) to a diet based on a mix of benthic (36.6% of sedimentary organic matter)
448 and pelagic (39.3% of mesozooplankton and 24.4% of small plankton) sources in period 2.
449 The same occurred in period 3, although the small plankton was the main food source
450 (69.2%), and sedimentary organic matter contribution decreased (27.0%). For the medusae,
451 small plankton was the only food source (100%) in period 1, but the diet changed in period 2,
452 including mainly sedimentary organic matter (64.3%) and mesozooplankton (32.3%). As the
453 isotopic signatures of the ephyrae collected in January 2018 were very similar to those of the
454 scyphistomae in the same period, their diet probably mainly consist of small plankton
455 organisms.
456
457 *Intra- and interspecific competitions for the food resources*

458 Intraspecific isotopic niche overlap was substantial during the whole period of co-occurrence
459 of the benthic and pelagic stages of *A. coerulea* in the lagoon (March to June; Fig. 9). Indeed,
460 although the percentage of niche overlap was higher in period 1 (41.5%) than in period 2
461 (only 9.9%), the isotopic niche of the medusae entirely overlaid that of the scyphistomae in
462 period 2. Similarly, although only three ephyrae samples were analysed in this study (all from
463 January 2018), their isotopic signatures were close to those observed for the scyphistomae in
464 period 1, suggesting high (although not quantifiable) trophic niche overlap among these two
465 life stages.
466 In Thau, interspecific trophic competition between *A. coerulea* and bivalves was observed,
467 although limited. The $\delta^{13}C$ and $\delta^{15}N$ signatures of the oysters from the lagoon varied from –
468 25.6 to –18.5 ‰ and from 8.4 to 9.4‰, respectively (Fig. 10). Significant differences in
469 isotopic signatures were observed between cultivated and wild individuals (PERMANOVA,
470 Pseudo-F_{11} = 12.4, p-value < 0.01; Fig. 10), with the former showing significantly higher $\delta^{13}C$
471 (–19.7 ± 0.9 ‰) and lower $\delta^{15}N$ (8.6 ± 0.3 ‰) signatures on average than the later (–20.1 ±
472 0.4 ‰ and 9.2 ± 0.3 ‰, respectively). Interspecific isotopic niche overlaps were limited
473 (<30%) and lower than that between cultivated and wild oysters (35.4%). Interspecific
474 isotopic niche overlap was more important between cultivated oysters and *A. coerulea* medusa
475 stage (29.1%). However, if we assume that the seasonal shifts in isotopic signatures are
476 consistent among years for both the jellyfish and the oysters, the trophic competition for food
477 should only occur at a limited period of the year and only with the medusae stage. Indeed,
478 only the signatures recorded in period 2 were responsible for the interspecific niche overlap
479 observed among *A. coerulea* medusae and cultivated (21.8%) or wild (21.1%) oysters.
480

481 **Discussion**

To our knowledge, this is the first study to investigate the trophic ecology of both the benthic and the pelagic stages of a jellyfish species (*A. coerulea*) in association with its in situ population dynamics and the plankton availability. The results obtained offer the unprecedented opportunity to identify the bottom-up processes regulating *A. coerulea* populations, contributing to our understanding of the formation of its blooms.

Trophic ecology of the pelagic stages of A. coerulea

Ephyrae were only collected once during the study period and their isotopic signature was similar to that of scyphistomae at the same time, indicating major importance of the small planktonic organic matter (i.e. phytoplankton and microzooplankton) in their diet. This result will have to be confirmed because, in Thau, *A. coerulea* ephyrae are mainly released in November, but strobilation continues until April (Marques et al. 2019). Therefore, we cannot exclude that the ephyrae caught in January 2018 had been released just a few days or weeks before their collection and therefore still had the isotopic signature of the scyphistomae that produced them. Moreover, because of their very low growth rate during the winter (< 0.1 $mm.day^{-1}$, Marques et al. 2015b), the ephyrae caught in January might not have yet incorporated the signature of the prey ingested after their release (Frazer et al. 1997). Nevertheless, phytoplankton, microzooplankton (such as rotifers) and suspended particulate organic matter have all been previously identified as important food sources for ephyrae (Båmstedt et al. 2001; Zheng et al. 2015) so our findings are in agreement with the literature. The results from medusae gut contents analysis support previous reports describing *A. coerulea* medusae as mesozooplanktivorous, feeding mainly on copepods and nauplii (mainly of cirripeds). Indeed, *Aurelia* spp. medusae have been suggested to prey mainly on mesozooplankton and to have higher clearance rates and selective preferences for crustacean prey such as copepods, cirriped nauplii, and cladocerans (Hansson 2006; Lo and Chen 2008).

507 Phytoplankton and microzooplankton also contributed to the diet of *A. coerulea* medusae in
508 Thau, but only during their first two months of growth and with low relative importance.
509 Indeed, *Aurelia* spp. diet often echoes prey local abundances in their environment (e.g. Ishii
510 and Tanaka 2001), which might explain these results, since the abundance of
511 microzooplankton and phytoplankton in the lagoon were higher in April and May. Yet,
512 variations of prey availability in Thau were not entirely reflected in *A. coerulea* medusae diet,
513 since mesozooplankton represented consistently more than 80% of the prey identified in their
514 guts, despite its lower in situ abundance in this period. Although gut content analyses
515 provided important qualitative information on the diet of jellyfish medusae, conclusions
516 regarding the importance of each prey type for their growth, at longer time scales, should be
517 drawn with caution, due to the bias associated with this technique. The digestion time of
518 mesozooplankton in the medusae guts might vary between 1 and 5h, depending on medusa
519 size, temperature, and prey type (Ishii and Tanaka 2001; Martinussen and Båmstedt 2001),
520 with smaller prey being digested faster (Martinussen and Båmstedt 2001). Therefore, gut
521 content analysis often leads to an overestimation of the importance of hard and big prey in the
522 diet, such as crustaceans. This might have contributed to a general overlook of the potential
523 relevance of the lower trophic levels to the diet of jellyfish (Javidpour et al. 2016). Indeed, in
524 Thau, the diet composition of *A. coerulea* medusae differed between gut content and stable
525 isotope analyses. The later approach underlined not only the importance of the phytoplankton
526 and microzooplankton (pooled as small plankton) for the diet of *A. coerulea* medusae in Thau
527 but also that of the sedimentary organic matter.
528 The diet of the *A. coerulea* medusae varied over time. In general, the $\delta^{13}C$ (–23.4 to –19.4‰)
529 and $\delta^{15}N$ (8.1 to 8.9‰) values found for the *A. coerulea* medusae stage were in the range of
530 the values published by Fleming et al. (2015) (–20.3 to –18.1 for $\delta^{13}C$ and 8.5 to 11.8 for
531 $\delta^{15}N$) and D'Ambra et al. (2013) (–20.5 ± 0.3‰ and 7.2 ± 0.4‰ on average for $\delta^{13}C$ and

532 $\delta^{15}N$, respectively). However, intra-annual fluctuations in medusae isotopic signatures
533 revealed a significant shift in May, with an increase of ca. 3.5 and 1‰ for $\delta^{13}C$ and $\delta^{15}N$,
534 respectively. This separates two distinct periods of stable isotopic signatures: period 1, during
535 medusae growth from March to April, and period 2, in June, when they reproduce before the
536 collapse of the bloom. This variation in the isotopic signature might indicate a rapid ontogenic
537 shift in the diet of the medusae, reflecting the change from small plankton to
538 mesozooplankton and sedimentary organic matter sources. A similar shift in the trophic niche
539 was also shown for *Aurelia aurita* in Northern Ireland, where medusae fed on higher trophic
540 levels by the end of their growing period (Fleming et al. 2015). Temporal variations in
541 isotopic signatures of predators might also reflect analogous changes in the isotopic signatures
542 at the base of the food webs (Post 2002). In this study, the values of the assessed organic
543 matter sources agree with those previously reported in Thau (Pernet et al. 2012) and other
544 north-western Mediterranean coastal lagoons (Dierking et al. 2012; Escalas et al. 2015) but
545 revealed significant fluctuations over time. In Thau, ^{13}C-depleted coastal inputs are dependent
546 on the rainfall, which was high in March and low in April (http://www.meteofrance.fr/climat-
547 passe-et-futur/bilans-climatiques/bilan-2017. Accessed 27 Jul 2019), likely contributing to the
548 variation in the $\delta^{13}C$ isotopic signatures of the lower trophic levels and then reflected in those
549 of *A. coerulea* medusae. However, similar trends were not observed for $\delta^{15}N$ isotopic
550 signatures, which showed a decreasing trend for most organic matter sources in May,
551 contrasting with an increasing trend for medusae in June. This underlines that the observed
552 isotopic niche shift for *A. coerulea* medusae was not only a reflection of temporal fluctuations
553 in the signatures of their prey but likely induced by a significant change in their diet. Finally,
554 our results highlight the importance of sedimentary organic matter (64.3%) in the diet of *A.*
555 *coerulea* medusae, as previously observed for *A. aurita* in the Kiel Fjord (Javidpour et al.
556 2016). Like most shallow marine ecosystems, the Thau lagoon is recurrently subjected to

sediment resuspension, triggered by river floods and strong wind activity (Fouilland et al. 2012). With this regard, the unidentified masses of organic matter found in the guts of the medusae were probably aggregates of re-suspended sedimentary organic matter.

Trophic ecology of the benthic stage of A. coerulea

The temporal variability of the $\delta^{13}C$ and $\delta^{15}N$ signatures of *A. coerulea* scyphistomae suggested two significant intra-annual shifts in their diet and identified three different isotopic niche periods. The diet of scyphistomae was mostly based on small plankton during period 1, included all available food sources during period 2 and changed to a mix of pelagic (i.e., small plankton) and sedimentary organic matter during period 3. These seasonal variations agree with those of the availability of planktonic food sources in the lagoon, following the high abundances of phytoplankton and microzooplankton in periods 1 and 3 and that of mesozooplankton in period 2 (i.e., in June). Our results agree with the few existing reports on the diet of jellyfish scyphistomae, which suggested that they feed on small mesozooplankton species (e.g. copepods, cladocerans, and cirripeds nauplii; Östman 1997; Ikeda et al. 2017), as well as on microzooplankton and phytoplankton (dinoflagellates, ciliates, rotifers, and diatoms; Kamiyama 2013; Wang et al. 2015; Huang et al. 2015). However, as for medusae, the temporal variation in scyphistomae isotopic signatures might also reflect the origin of the carbon and nitrogen inputs in the lagoon (Post 2002). Indeed, fluctuations in $\delta^{13}C$ and $\delta^{15}N$ values might reflect the stronger contribution of terrestrial inputs to the basis of the food web, after rainy events in period 1 (Vizzini et al. 2005; Pernet et al. 2012a) and the exceptionally low terrestrial inputs from June onwards (periods 2 and 3), due to a very dry summer and autumn in 2017 (> 80% loss of rainfall when compared with the mean between 1981 – 2010 in October, http://www.meteofrance.fr/climat-passe-et-futur/bilans-climatiques/bilan-2017. Accessed 27 Jul 2019). Furthermore, it might also be affected by the higher influence of

582 wastewater effluent in the lagoon during dry periods (Perrin and Tournoud 2009), which is
583 suggested to induce an enrichment of $\delta^{15}N$ signatures, as in other coastal lagoons (Vizzini et
584 al. 2005; Dierking et al. 2012; Escalas et al. 2015). Yet, the skewed temporal pattern of the
585 scyphistomae isotopic signatures when compared with their sources further confirm a
586 seasonal variation in their diet.
587 The increase in mesozooplankton consumption during period 2, when the abundance of this
588 prey is maximal, is not surprising. Higher abundances of this type of prey (especially of newly
589 hatched *Artemia* sp.) is recognized to induce better performances of scyphistomae (i.e.,
590 growth, asexual reproduction, and strobilation) in laboratory experiments (e.g. Ikeda et al.
591 2017; Hubot et al. 2017). However, our results further highlight the prominent role of the
592 lower trophic levels in the feeding and benthic population dynamics of the species in Thau.
593 Although we were not able to precisely quantify the relative importance of phytoplankton and
594 microzooplankton in the diet of *A. coerulea* scyphistomae, they both appear to be important.
595 Phytoplankton cells are seemingly insufficient to support scyphistomae basic metabolic rates
596 at high temperatures (20ºC) and for long periods (Wang et al. 2015; Huang et al. 2015), but
597 they provide a suitable alternative source of energy for their survival and asexual reproduction
598 at low temperatures (Huang et al. 2015; Wang et al. 2015). Therefore, peaks in phytoplankton
599 abundances during period 1 probably support *A. coerulea* scyphistomae survival over the
600 winter and early spring. Similarly, the significant positive correlation between the abundance
601 of microzooplankton and the percentage of scyphistomae producing buds suggests that this
602 type of prey promotes the buds production, ultimately driving the benthic population density.
603 Indeed, buds production by scyphistomae of *Aurelia aurita* has been previously shown to
604 increase when reared on a ciliate-based diet rather than on the larger *Artemia* prey (Kamiyama
605 2013). Interestingly, although more buds were produced in April in the lagoon (due to high
606 scyphistomae density) the peak of the percentage of scyphistomae producing buds, as well as

607 the maximum number of buds per scyphistoma, were registered in September (Marques et al.
608 2019), co-occurring with high abundances of microzooplankton in the lagoon.
609 Lastly, as for medusae, our results highlight the importance of the sedimentary organic matter
610 in the diet of *A. coerulea* scyphistomae in Thau. This does not come as a major surprise
611 because re-suspended sediments were often observed on the scyphistomae samples collected
612 *in situ*. Sedimentary organic matter is usually composed by a mixture of microphytobenthos,
613 heterotrophic microorganisms (bacteria, ciliates, protozoans, nematodes) and detritus,
614 classically associated and re-suspended with sediment (Dubois et al. 2007), which might
615 provide a suitable source of food for jellyfish benthic stages (Östman 1997).
616
617 *Intra- and interspecific competition*
618 The benthic scyphistomae and the pelagic medusae of *A. coerulea*, although inhabiting
619 different habitats, appeared to share, at least partially, the same organic matter sources in the
620 lagoon. During period 1, their high isotopic niche overlap, and the results of the mixing
621 models, indicate that both stages feed on phytoplankton and/or microzooplankton. In period 2,
622 despite a lower isotopic niche overlap, the trophic niche of the medusae entirely covers that of
623 the scyphistomae. This suggests that during large medusae blooms and under food limitation
624 conditions, intraspecific competition for food might occur in the lagoon, with possible
625 detrimental impacts on the scyphistomae population.
626 One of the main concerns regarding the presence of *A. coerulea* in Thau is the potential
627 competition for food with the oysters produced in the lagoon, in particular during the medusae
628 blooms and due to the overspread distribution of scyphistomae (Marques et al. 2015a).
629 However, our results suggest only a limited trophic niche overlap. Although oysters and *A.*
630 *coerulea* stages were not collected in the same year (except in period 3) we assumed that the
631 isotopic signature of the oysters mostly varies intra-annually (Pernet et al. 2012). If this is

true, our results indicate that interspecific competition for food only potentially occurs between *A. coerulea* medusae and oysters (cultivated and wild) in period 2. During this period, sedimentary organic matter was an important source in the diet of *A. coerulea* medusae and also reported as part of the diet of oysters (Dubois and Colombo 2014). This might explain the isotopic niche overlap, although restricted, between these two organisms at this period. The limited interspecific trophic competition between the *A. coerulea* and the oysters might result from their different filtration and particle retention mechanisms, as previously suggested for other suspension-feeding species co-occurring with oysters (Dubois and Colombo 2014). Indeed, *A. coerulea* medusae are cruising predators, capturing their prey using locally generated flow currents (Dabiri et al. 2005) and the scyphistomae use a passive ambush strategy (Huang et al. 2015), contrasting with the true filter-feeding strategy of the oysters (Dubois et al. 2007; Dubois and Colombo 2014). The different mechanisms to capture prey, likely promoted the selection and ingestion of different organic matter sources, reducing the trophic competition for the same type of prey. Phytoplankton (especially diatoms) is the main source of food for oysters (Dupuy et al. 2000; Pernet et al. 2012). In situ feeding experiments showed that the consumption of *Aurelia* sp. medusae on micro- and mesozooplankton organisms released the predation pressure from these secondary producers on the lower trophic levels, boosting phytoplankton biomass and bacterial production (Turk et al. 2008). Therefore, it is possible that the blooms of *A. coerulea* medusae might even be advantageous for the production of oysters in the lagoon, via a top-down cascade effect on the microbial community.

Bottom-up control of the A. coerulea population dynamics

In the Thau lagoon, the winter and early spring are critical periods for the formation of the *A. coerulea* bloom (Marques et al. 2019). The production of ephyrae occurs between

November and April, with two main peaks: in November (during period 3) due to a high percentage of the scyphistomae strobilating (despite their low densities), and in February – March (during period 1), when this percentage is low but the density of scyphistomae is high (Marques et al. 2019). As they grow to become medusae, the magnitude of the bloom is thus, tightly dependent on the accumulated production of ephyrae, their survival, and growth rate. In period 1, phytoplankton and microzooplankton are the main sources of food for both the ephyrae and scyphistomae of *A. coerulea*. This stresses the role of the lower trophic levels in the formation of the local jellyfish blooms: they promote higher levels of scyphistomae and ephyrae survival and they boost the production of buds, leading to higher scyphistomae densities and ephyrae production. In summer (during period 2) both *A. coerulea* life stages change their diet to a mix of all sources (except small plankton for medusae). This is particularly important because it supports the peak of the bloom, following high growth rates of medusae, as well as their sexual reproduction (Fig. 11; Marques et al. 2015b). It is also during this period that scyphistomae coverage declines (Fig. 11, Marques et al. 2019). Our results suggest a potentially high intraspecific trophic competition between scyphistomae and medusae, especially during this period. Therefore, the high abundance and high predation pressure of the medusae might lead to the reduction of food availability for scyphistomae and could contribute to the reduction of their coverage. During the following dry season (i.e., period 3), a bacteria-based food web prevails in the lagoon, with internal regeneration of nitrogen, due to the absence of terrestrial freshwater inputs in the lagoon (Chapelle et al. 2000). This likely supports the peaks of microzooplankton abundance since these organisms are recognized as important bacterivorous (Rassoulzadegan and Sheldon 1986). Microzooplankton appear to have a critical role as a source of food for scyphistomae, which, in period 3, would sustain not only the noticed peak of buds production in September but also

681 the main strobilation period in November (Marques et al. 2019), i.e., the first peak of ephyrae
682 production and the initial foundation of the subsequent jellyfish bloom in the Thau lagoon.
683
684 *Limitation of the study*
685 Although stable isotope analysis is a powerful tool to assess the trophic ecology of predators,
686 the MixSIAR results should be considered with caution. Indeed, mixing models always
687 provide a solution but their results might not always be biologically relevant: their precision
688 decreases with the number of introduced organic matter sources and depends greatly on the
689 accuracy of their signatures (Dubois et al. 2007).
690 In this work, we used a turnover time of one month for both jellyfish life stages, following the
691 results reported for *Aurelia* sp. (18 – 20 days, D'Ambra et al. 2014). If inaccurate, this might
692 have significantly biased the MixSIAR results for each isotopic niche period because the set
693 of organic matter source signatures matching with those of the jellyfish might be incorrect.
694 Moreover, despite the frequency of sampling for organic matter sources during our study,
695 some periods of the year (e.g. July – September) were less represented in the database. Given
696 the intra-annual variability in the isotopic signatures of the plankton component, we cannot
697 fully exclude that this sampling gap slightly biased our results.
698 The implementation of different isotopic fractionation values in the mixing models also
699 drastically modify their final results. In our study, using the fractionation values proposed by
700 D'Ambra et al. (2014) would result in a higher contribution of mesozooplankton to the diet in
701 both stages of *A. coerulea*. However, the values from D'Ambra et al. (2014) are very different
702 from those typically reported in the literature (e.g. Vander Zanden and Rasmussen 2001; Post
703 2002), leading to unrealistic trophic levels (Fleming et al. 2015; Milisenda et al. 2018).
704 Furthermore, the temperature (which is highly variable in Thau), the feeding condition, the

sexual maturity (e.g. Barnes et al. 2007), and, probably, the life stage might also affect fractionation and turnover values.

Conclusion

Knowledge of the trophic ecology and population dynamics of jellyfish is imperative to understand the main environmental drivers of blooms. With this regard, the Thau lagoon offered an exceptional framework to study both benthic and pelagic trophic interactions and to uncover the main organic matter sources supporting key periods of the *A. coerulea* life cycle. In particular, we highlight the role of phytoplankton and microzooplankton in supporting scyphistomae survival and asexual reproduction, that of mesozooplankton and sedimentary organic matter for the growth of medusae, as well as the possible negative influence of intraspecific competition on the benthic population dynamics. Moreover, we demonstrate that the interspecific trophic competition between *A. coerulea* and the commonly cultivated oyster *C. gigas* is likely to be limited, at least in the Thau lagoon, and therefore, we advocate that *A. coerulea* blooms have a seemingly restricted impact on the local shellfish production.

727 **References:**

728 Anderson MJ (2017) Permutational Multivariate Analysis of Variance (PERMANOVA). In:
729 Wiley StatsRef: Statistics Reference Online. John Wiley & Sons, Ltd, Chichester, UK,
730 pp 1–15. doi: 10.1002/9781118445112.stat07841

731 Båmstedt U, Wild B, Martinussen MB (2001) Significance of food type for growth of ephyrae
732 *Aurelia aurita* (Scyphozoa). Mar Biol 139:641–650. doi: 10.1007/s002270100623

733 Barnes C, Sweeting CJ, Jennings S, Barry JT, Polunin NVC (2007) Effect of temperature and
734 ration size on carbon and nitrogen stable isotope trophic fractionation. Funct Ecol
735 21:356–362. doi: 10.1111/j.1365-2435.2006.01224.x

736 Boero F, Bouillon J, Gravili C, Miglietta MP, Parsons T, Piraino S (2008) Gelatinous
737 plankton: irregularities rule the world (sometimes). Mar Ecol Prog Ser 356:299–310. doi:
738 10.3354/meps07368

739 Bonnet D, Molinero J-C, Schohn T, Daly-Yahia MN (2012) Seasonal changes in the
740 population dynamics of *Aurelia aurita* in Thau lagoon. Cah Biol Mar 53:343–347.

741 Boyer S, Bouvy M, Bonnet D (2013) What triggers *Acartia* species egg production in a
742 Mediterranean lagoon? Estuar Coast Shelf Sci 117:125–135. doi:
743 10.1016/j.ecss.2012.11.006

744 Chapelle A, Ménesguen A, Deslous-Paoli J-M, Souchu P, Mazouni N, Vaquer A, Millet B
745 (2000) Modelling nitrogen, primary production and oxygen in a Mediterranean lagoon.
746 Impact of oysters farming and inputs from the watershed. Ecol Modell 127:161–181. doi:
747 10.1016/S0304-3800(99)00206-9

748 Condon RH, Graham WM, Duarte CM, Pitt KA, Lucas CH, Haddock SHD, Sutherland KR,
749 Robinson KL, Dawson MN, Decker MB, Mills CE, Purcell JE, Malej A, Mianzan H,
750 Uye S-I, Gelcich S, Madin LP (2012) Questioning the Rise of Gelatinous Zooplankton in
751 the World's Oceans. Bioscience 62:160–169. doi: 10.1525/bio.2012.62.2.9

752 D’Ambra I, Graham WM, Carmichael RH, Malej A, Onofri V (2013) Predation patterns and
753 prey quality of medusae in a semi-enclosed marine lake: implications for food web
754 energy transfer in coastal marine ecosystems. J Plankton Res 35:1305–1312. doi:
755 10.1093/plankt/fbt065
756 D’Ambra I, Carmichael RH, Graham WM (2014) Determination of $\delta^{13}C$ and $\delta^{15}N$ and trophic
757 fractionation in jellyfish: Implications for food web ecology. Mar Biol 161:473–480. doi:
758 10.1007/s00227-013-2345-y
759 Dabiri JO, Colin SP, Costello JH, Gharib M (2005) Flow patterns generated by oblate
760 medusan jellyfish: field measurements and laboratory analyses. J Exp Biol 208:1257 LP
761 – 1265. doi: 10.1242/jeb.01519
762 Dawson MN, Martin DL (2001) Geographic variation and ecological adaptation in *Aurelia*
763 *aurita* (Scyphozoa, Semaestomeae): some implications from molecular phylogenetics.
764 Hydrobiologia 451:259–273. doi: https://doi.org/10.1023/A:1011869215330
765 Dierking J, Morat F, Letourneur Y, Harmelin-Vivien M (2012) Fingerprints of lagoonal life:
766 Migration of the marine flatfish *Solea solea* assessed by stable isotopes and otolith
767 microchemistry. Estuar Coast Shelf Sci 104–105:23–32. doi: 10.1016/j.ecss.2011.03.018
768 Dubois S, Orvain F, Marin-Léal JC, Ropert M, Lefebvre S (2007) Small-scale spatial
769 variability of food partitioning between cultivated oysters and associated suspension-
770 feeding species, as revealed by stable isotopes. Mar Ecol Prog Ser 336:151–160. doi:
771 10.3354/meps336151
772 Dubois SF, Colombo F (2014) How picky can you be? Temporal variations in trophic niches
773 of co-occurring suspension-feeding species. Food Webs 1:1–9. doi:
774 10.1016/j.fooweb.2014.07.001
775 Dupuy C, Vaquer A, Lam-Höai T, Rougier C, Mazouni N, Lautier J, Collos Y, Le Gall S
776 (2000) Feeding rate of the oyster *Crassostrea gigas* in a natural planktonic community of

777 the Mediterranean Thau Lagoon. Mar Ecol Prog Ser 205:171–184. doi:
778 10.3354/meps205171
779 Escalas A, Ferraton F, Paillon C, Vidy G, Carcaillet F, Salen-Picard C, Le Loc'h F, Richard
780 P, Darnaude AM (2015) Spatial variations in dietary organic matter sources modulate the
781 size and condition of fish juveniles in temperate lagoon nursery sites. Estuar Coast Shelf
782 Sci 152:78–90. doi: 10.1016/j.ecss.2014.11.021
783 Fleming NEC, Harrod C, Newton J, Houghton JDR (2015) Not all jellyfish are equal: isotopic
784 evidence for inter- and intraspecific variation in jellyfish trophic ecology. PeerJ 3:e1110.
785 doi: 10.7717/peerj.1110
786 Fouilland E, Trottet A, Bancon-Montigny C, Bouvy M, Le Floc'h E, Gonzalez J-L, Hatey E,
787 Mas S, Mostajir B, Nouguier J, Pecqueur D, Rochelle-Newall E, Rodier C, Roques C,
788 Salles C, Tournoud M-G, Vidussi F (2012) Impact of a river flash flood on microbial
789 carbon and nitrogen production in a Mediterranean Lagoon (Thau Lagoon, France).
790 Estuar Coast Shelf Sci 113:192–204. doi: 10.1016/j.ecss.2012.08.004
791 Frazer TK, Ross RM, Quetin LB, Montoya JP (1997) Turnover of carbon and nitrogen during
792 growth of larval krill, *Euphausia superba* Dana: a stable isotope approach. J Exp Mar
793 Bio Ecol 212:259–275. doi: 10.1016/S0022-0981(96)02740-2
794 Han C-H, Uye S-I (2010) Combined effects of food supply and temperature on asexual
795 reproduction and somatic growth of polyps of the common jellyfish *Aurelia aurita* s.l.
796 Plankt Benthos Res 5:98–105. doi: 10.3800/pbr.5.98
797 Hansson LJ (2006) A method for in situ estimation of prey selectivity and predation rate in
798 large plankton, exemplified with the jellyfish *Aurelia aurita* (L.). J Exp Mar Bio Ecol
799 328:113–126. doi: 10.1016/j.jembe.2005.07.002
800 Huang XG, Huang B, Zeng Y, Li SX (2015) Effect of dinoflagellates and diatoms on the
801 feeding response and survival of *Aurelia* sp. polyps. Hydrobiologia 754:179–188. doi:

802 10.1007/s10750-014-2023-1
803 Hubot N, Lucas CH, Piraino S (2017) Environmental control of asexual reproduction and
804 somatic growth of *Aurelia* spp. (Cnidaria, Scyphozoa) polyps from the Adriatic Sea.
805 PLoS One 12:e0178482. doi: 10.1371/journal.pone.0178482
806 Ikeda H, Mizota C, Uye S-I (2017) Bioenergetic characterization in *Aurelia aurita* (Cnidaria:
807 Scyphozoa) polyps and application to natural polyp populations. Mar Ecol Prog Ser
808 568:87–100. doi: 10.3354/meps12055
809 Ishii H, Båmstedt U (1998) Food regulation of growth and maturation in a natural population
810 of *Aurelia aurita* (L.). J Plankton Res 20:805–816. doi: 10.1093/plankt/20.5.805
811 Ishii H, Tanaka F (2001) Food and feeding of *Aurelia aurita* in Tokyo Bay with an analysis of
812 stomach contents and a measurement of digestion times. In: Purcell JE, Graham WM,
813 Dumont HJ (eds) Jellyfish Blooms: Ecological and Societal Importance. Developments
814 in Hydrobiology, vol 155, Springer Netherlands, Dordrecht, pp 311–320. doi:
815 10.1007/978-94-010-0722-1_26
816 Jackson AL, Inger R, Parnell AC, Bearhop S (2011) Comparing isotopic niche widths among
817 and within communities: SIBER - Stable Isotope Bayesian Ellipses in R. J Anim Ecol
818 80:595–602. doi: 10.1111/j.1365-2656.2011.01806.x
819 Jaine AK (2010) Data clustering: 50 years beyond K-means Pattern Recognit Lett 31:651-
820 666. 10.1016/j.patrec.2009.09.011.
821 Javidpour J, Cipriano-Maack AN, Mittermayr A, Dierking J (2016) Temporal dietary shift in
822 jellyfish revealed by stable isotope analysis. Mar Biol 163:112. doi: 10.1007/s00227-
823 016-2892-0
824 Kamiyama T (2013) Planktonic ciliates as food for the scyphozoan *Aurelia aurita* (s.l.):
825 Effects on asexual reproduction of the polyp stage. J Exp Mar Bio Ecol 445:21–28. doi:
826 10.1016/j.jembe.2013.03.018

827 Kassambara A, Mundt F (2017) factoextra: Extract and Visualize the Results of Multivariate
828 Data Analyses. 1–74. R package version 1.0.5
829 Layman CA, Araujo MS, Boucek R, Hammerschlag-Peyer CM, Harrison E, Jud ZR, Matich
830 P, Rosenblatt AE, Vaudo JJ, Yeager LA, Post DM, Bearhop S (2012) Applying stable
831 isotopes to examine food-web structure: an overview of analytical tools. Biol Rev
832 87:545–562. doi: 10.1111/j.1469-185X.2011.00208.x
833 Lo WT, Chen IL (2008) Population succession and feeding of scyphomedusae, *Aurelia aurita*,
834 in a eutrophic tropical lagoon in Taiwan. Estuar Coast Shelf Sci 76:227–238. doi:
835 10.1016/j.ecss.2007.07.015
836 Lucas CH (1994) Biochemical composition of *Aurelia aurita* in relation to age and sexual
837 maturity. J Exp Mar Bio Ecol 183:179–192. doi: 10.1016/0022-0981(94)90086-8
838 Lucas CH (2001) Reproduction and life history strategies of the common jellyfish, *Aurelia*
839 *aurita*, in relation to its ambient environment. In: Purcell JE, Graham WM, Dumont HJ
840 (eds) Jellyfish Blooms: Ecological and Societal Importance. Developments in
841 Hydrobiology, vol 155, Springer Netherlands, Dordrecht, pp 229–246doi: 10.1007/978-
842 94-010-0722-1_19
843 Lucas CH, Hirst AG, Williams JA (1997) Plankton Dynamics and *Aurelia aurita* Production
844 in Two Contrasting Ecosystems: Comparisons and Consequences. Estuar Coast Shelf Sci
845 45:209–219. doi: 10.1006/ecss.1996.0173
846 Marques R, Cantou M, Soriano S, Molinero J-C, Bonnet D (2015a) Mapping distribution and
847 habitats of *Aurelia* sp. polyps in Thau lagoon, north-western Mediterranean sea (France).
848 Mar Biol 162:1441–1449. doi: 10.1007/s00227-015-2680-2
849 Marques R, Albouy-Boyer S, Delpy F, Carré C, Le Floc'H É, Roques C, Molinero J-C,
850 Bonnet D (2015b) Pelagic population dynamics of *Aurelia* sp. in French Mediterranean
851 lagoons. J Plankton Res 37:1019–1035. doi: 10.1093/plankt/fbv059

852 Marques R, Darnaude AM, Schiariti A, Tremblay Y, Molinero J-C, Soriano S, Hatey E,
853 Colantoni S, Bonnet D (2019) Dynamics and asexual reproduction of the jellyfish
854 *Aurelia coerulea* benthic life stage in the Thau lagoon (northwestern Mediterranean).
855 Mar Biol 166:74. doi: 10.1007/s00227-019-3522-4
856 Martinez Arbizu P (2019) pairwiseAdonis: Pairwise multilevel comparison using adonis. R
857 package, version 0.0.1.
858 Martinussen MB, Båmstedt U (2001) Digestion rate in relation to temperature of two
859 gelatinous planktonic predators. Sarsia 86:21–35. doi:
860 10.1080/00364827.2001.10420458
861 Milisenda G, Rossi S, Vizzini S, Fuentes VL, Purcell JE, Tilves U, Piraino S (2018) Seasonal
862 variability of diet and trophic level of the gelatinous predator *Pelagia noctiluca*
863 (Scyphozoa). Sci Rep 8:12140. doi: 10.1038/s41598-018-30474-x
864 Millet B, Cecchi P (1992) Wind-induced hydrodynamic control of the phytoplankton biomass
865 in a lagoon ecosystem. Limnol Oceanogr 37:140–146. doi: 10.4319/lo.1992.37.1.0140
866 Mills C (2001) Are population increasing globally in response to changing ocean conditions?
867 Hydrobiologia 451:55–68. doi: https://doi.org/10.1023/A:1011888006302
868 Mongruel R, Vanhoutte-Brunier A, Fiandrino A, Valette F, Ballé-Béganton J, Pérez Agúndez
869 JA, Gallai N, Derolez V, Roussel S, Lample M, Laugier T (2013) Why, how, and how
870 far should microbiological contamination in a coastal zone be mitigated? An application
871 of the systems approach to the Thau lagoon (France). J Environ Manage 118:55–71. doi:
872 10.1016/j.jenvman.2012.12.038
873 Morais P, Dias E, Cruz J, Chainho P, Angélico MM, Costa JL, Barbosa AB, Teodósio MA
874 (2017) Allochthonous-derived organic matter subsidizes the food sources of estuarine
875 jellyfish. J Plankton Res 39:870–877. doi: 10.1093/plankt/fbx049
876 Nixon SW (1995) Coastal marine eutrophication: A definition, social causes, and future

877 concerns. Ophelia 41:199–219. doi: 10.1080/00785236.1995.10422044
878 Oksanen J, Blanchet FG, Friendly M, Kindt R, Legendre P, Mcglinn D, Minchin PR, O'Hara
879 RB, Simpson GL, Solymos P, Stevens MHH, Szoecs E, Wagner H (2019) Vegan:
880 Community Ecology Package. R package, version 2.5-4
881 Östman C (1997) Abundance, feeding behaviour and nematocysts of scyphopolyps (Cnidaria)
882 and nematocysts in their predator, the nudibranch *Coryphella verrucosa* (Mollusca). In:
883 Naumov AD, Hummel H, Sukhotin AA, Ryland JS (eds) Interactions and Adaptation
884 Strategies of Marine Organisms. Springer Netherlands, Dordrecht, pp 21–28
885 Pernet F, Malet N, Pastoureaud A, Vaquer A, Quéré C, Dubroca L (2012) Marine diatoms
886 sustain growth of bivalves in a Mediterranean lagoon. J Sea Res 68:20–32. doi:
887 10.1016/j.seares.2011.11.004
888 Perrin J-L, Tournoud M-G (2009) Hydrological processes controlling flow generation in a
889 small Mediterranean catchment under karstic influence. Hydrol Sci J 54:1125–1140. doi:
890 10.1623/hysj.54.6.1125
891 Pinnegar JK, Polunin NVC (1999) Differential fractionation of $\delta^{13}C$ and $\delta^{15}N$ among fish
892 tissues: implications for the study of trophic interactions. Funct Ecol 13:225–231. doi:
893 10.1046/j.1365-2435.1999.00301.x
894 Pitt KA, Connolly RM, Meziane T (2009) Stable isotope and fatty acid tracers in energy and
895 nutrient studies of jellyfish: A review. Hydrobiologia 616:119–132. doi:
896 10.1007/s10750-008-9581-z
897 Plus M, La Jeunesse I, Bouraoui F, Zaldívar J-M, Chapelle A, Lazure P (2006) Modelling
898 water discharges and nitrogen inputs into a Mediterranean lagoon: Impact on the primary
899 production. Ecological Modelling 193:69–89. doi:10.1016/j.ecolmodel.2005.07.037
900 Post DM (2002) Using stable isotopes to estimate trophic position: models, methos, and
901 assumptions. . Ecology 83:703–718. doi: Doi 10.2307/3071875

902 Post DM, Layman CA, Arrington DA, Takimoto G, Quattrochi J, Montaña CG (2007) Getting
903 to the fat of the matter: Models, methods and assumptions for dealing with lipids in
904 stable isotope analyses. Oecologia 152:179–189. doi: 10.1007/s00442-006-0630-x
905 Purcell JE (2012) Jellyfish and Ctenophore Blooms Coincide with Human Proliferations and
906 Environmental Perturbations. Ann Rev Mar Sci 4:209–235. doi: 10.1146/annurev-
907 marine-120709-142751
908 Rassoulzadegan F, Sheldon RW (1986) Predator-prey interactions of nanozooplankton and
909 bacteria in an oligotrophic marine environment. Limnol Oceanogr 31:1010–1029. doi:
910 10.4319/lo.1986.31.5.1010
911 Stock BC, Semmens BX (2016) MixSIAR GUI User Manual. Version 3.1 1–42. doi:
912 10.5281/zenodo.47719
913 Syväranta J, Rautio M (2010) Zooplankton, lipids and stable isotopes: importance of seasonal,
914 latitudinal, and taxonomic differences. Can J Fish Aquat Sci 67:1721–1729. doi:
915 10.1139/F10-091
916 Turk V, Lučić D, Flander-Putrle V, Malej A (2008) Feeding of *Aurelia* sp. (Scyphozoa) and
917 links to the microbial food web. Mar Ecol 29:495–505. doi: 10.1111/j.1439-
918 0485.2008.00250.x
919 Utermöhl H (1958) Zur Vervollkommnung der quantitativen Phytoplankton-Methodik. SIL
920 Commun 1953-1996 9:1–38. doi: 10.1080/05384680.1958.11904091
921 Wang Y-T, Zheng S, Sun S, Zhang F (2015) Effect of temperature and food type on asexual
922 reproduction in *Aurelia* sp.1 polyps. Hydrobiologia 754:169–178. doi: 10.1007/s10750-
923 014-2020-4
924 Yokoyama H, Tamaki A, Harada K, Shimoda K, Koyama K, Ishihi Y (2005) Variability of
925 diet-tissue isotopic fractionation in estuarine macrobenthos. Mar Ecol Prog Ser 296:115–
926 128. doi: 10.3354/meps296115

927 Vander Zanden MJ, Rasmussen JB (2001) Variation in $\delta^{15}N$ and $\delta^{13}C$ trophic fractionation:
928 Implications for aquatic food web studies. Limnol Oceanogr 46:2061–2066. doi:
929 10.4319/lo.2001.46.8.2061
930 Zheng S, Sun X, Wang Y, Sun S (2015) Significance of different microalgal species for
931 growth of moon jellyfish ephyrae, *Aurelia* sp.1. J Ocean Univ China 14:823–828. doi:
932 10.1007/s11802-015-2775-x
933 Zuur AF, Ieno EN, Walker NJ, Saveliev AA, Smith GM (2009) Mixed Effects Models and
934 Extensions in Ecology with R. Springer New York
935
936
937
938
939

Acknowledgment:

We would like to thank Solenn Soriano, Nicolas Nouguier, and Remy Valdes for their technical support during SCUBA dives and fieldwork. We also thank Sandrine Crochemore and Sébastien Colantoni for their assistance during laboratory samples preparation. We thank Simon Julien from *huitres-bouzigues.com* for providing the cultivated oyster samples. Plankton diversity and abundance data are part of a long-term monitoring program on microbial communities in the Thau lagoon funded by *Observatoire des Sciences de l'Univers OREME* (OSU-OREME). Data are available on (https://data.oreme.org/plankton/plankton_thau_home). The laboratory analysis of samples to determine stable isotope signatures was performed at the Stable Isotope Facility at the University of California, Davis, USA. The authors declare that they have no conflict of interests.

Tables

Table 1: Frequency of occurrence (FO), index of relative importance (IRI) and mean abundance of prey items found in *A. coerulea* medusae gut contents during the period of its presence in the Thau lagoon. Numbers in parenthesis are the number of medusae with prey items analyzed.

	FO (%)			IRI (%)			Abundance (± SD) (ind.medusae^{-1})		
Prey	**Apr (5)**	**May (9)**	**Jun (8)**	**Apr (5)**	**May (9)**	**Jun (8)**	**Apr (5)**	**May (9)**	**Jun (8)**
Phytoplankton	20.0	33.3	0.0	3.4	5.6	0.0	1.0 (2.2)	1.0 (1.8)	0.0 (0.0)
Microzooplankton	60.0	55.6	0.0	7.5	12.5	0.0	2.2 (3.8)	2.2 (3.4)	0.0 (0.0)
Mesozooplankton (total)	80.0	88.9	100	89.1	81.9	100	26.2 (35.4)	14.6 (13.4)	10.3 (18.3)
- *Copepods*	40.0	66.7	87.5	34.7	21.9	46.3	10.2 (20.1)	3.9 (5.7)	4.8 (9.9)
- *Nauplii (copepods and cirripeds)*	60.0	88.9	62.5	4.8	31.3	41.5	1.4 (2.1)	5.6 (8.5)	4.3 (7.8)
- *Other crustaceans*	20.0	55.6	50.0	0.7	10.0	8.5	0.2 (0.4)	1.8 (3.5)	0.9 (1.1)
- *Non-crustaceans*	60.0	66.7	25.0	49.0	18.8	3.7	14.4 (20.9)	3.3 (4.5)	0.4 (0.7)

Table 2: Parameters of the generalized linear models used to assess correlations between the benthic population dynamics variables (scyphistomae coverage and scyphistomae producing buds) with the abundance [ln (x+1)] of phytoplankton (cell L^{-1}), microzooplankton (cell L^{-1}) and mesozooplankton (ind m^{-3}).

	Estimate	**Std. Error**	**t value**	**p-value**
Scyphistomae coverage (%)				
(Intercept)	-0.17	0.07	-2.46	0.03
Phytoplankton	0.02	0.01	2.97	**0.01**
Microzooplankton	0.01	0.01	2.10	0.05
Mesozooplankton	0.00	0.00	0.02	0.98
Scyphistomae producing buds (%)				
(Intercept)	-3.82	0.35	-10.95	< **0.01**
Phytoplankton	-0.01	0.03	-0.47	0.64
Microzooplankton	0.26	0.03	10.19	< **0.01**
Mesozooplankton	0.00	0.02	-0.09	0.93

965 Table 3: Stable $\delta^{13}C$ and $\delta^{15}N$ isotope signatures (mean ± SD) of *A. coerulea* and organic
966 matter sources used in MixSIAR model for each isotopic niche period. Sources A are the
967 values of organic matter sources used for scyphistomae models, including all data, while
968 Sources B are the values of organic matter sources collected from February to May, used for
969 medusae models. *n* is the number of samples used to calculate each mean. SP: small plankton;
970 Mesoz.: mesozooplankton; SOM: sedimentary organic matter.

	Period 1			**Period 2**			**Period 3**		
	$\delta^{13}C$ (± SD) ‰	**$\delta^{15}N$ (± SD) ‰**	***n***	**$\delta^{13}C$ (± SD) ‰**	**$\delta^{15}N$ (± SD) ‰**	***n***	**$\delta^{13}C$ (± SD) ‰**	**$\delta^{15}N$ (± SD) ‰**	***n***
Scyphistomae	-22.8 (0.4)	8.0 (0.5)	18	-19.3 (0.2)	9.0 (0.1)	9	-21.1 (0.3)	8.5 (0.4)	9
Medusae	-23.4 (0.7)	8.1 (0.3)	13	-19.4 (0.5)	8.9 (0.3)	7			
Sources A									
SP	-22.1 (2.0)	6.5 (0.3)	18	-20.6 (0.8)	6.2 (0.7)	22	-21.0 (0.9)	6.7 (0.3)	6
Mesoz.	-22.9 (0.9)	8.0 (0.4)	9	-19.2 (0.7)	7.4 (0.3)	12	-20.1 (0.1)	7.5 (0.0)	3
SOM	-20.2 (0.9)	5.5 (0.3)	6	-20.6 (0.1)	5.4 (0.2)	6	-20.7 (0.0)	5.3 (0.0)	2
Sources B									
SP	-23.3 (0.9)	6.4 (0.3)	12	-20.9 (0.5)	5.8 (0.3)	15			
Mesoz.	-23.4 (0.3)	8.2 (0.2)	6	-18.8 (0.2)	7.3 (0.3)	9			
SOM	-18.9 (0.0)	5.8 (0.1)	2	-20.5 (0.0)	5.6 (0.0)	2			

971

972

973 **Figures**

974

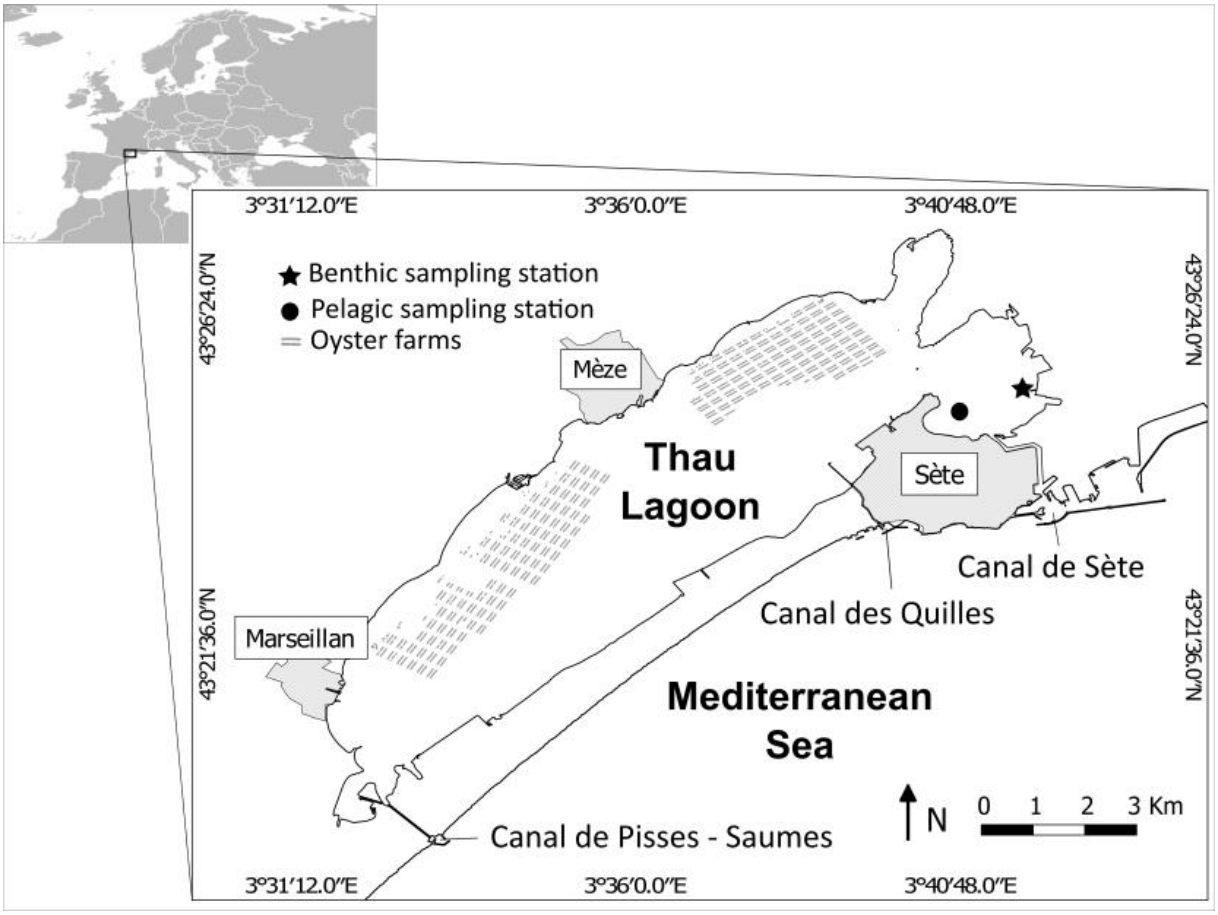

975

976 Fig. 1: Map of the Thau lagoon showing the location of the benthic (star) and pelagic (dot)
977 sampling stations for this study. Shaded areas represent urban zones and grey points represent
978 oyster farms.

979

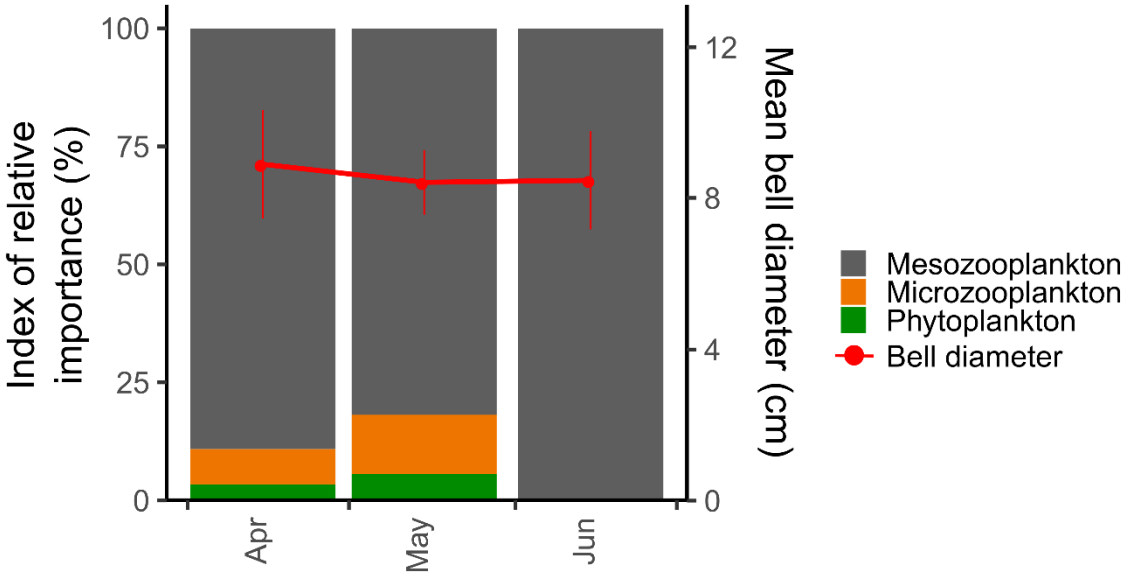

980

981 Fig. 2: Index of relative importance of the three main prey groups found in the guts of *A.*

982 *coerulea* medusae and the bell diameter of all individuals collected for gut content analysis.

983

984

985

986

987

988

989

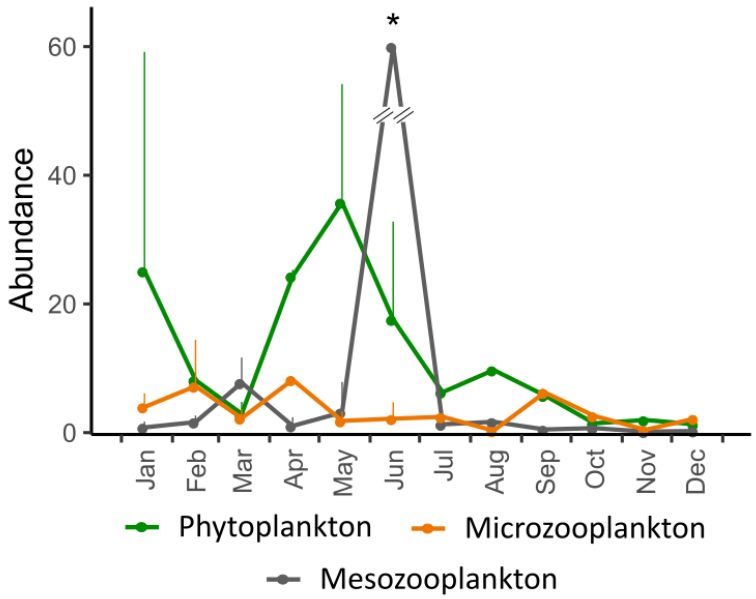

990

991 Fig. 3: Temporal variability of phytoplankton (x10^3 cell L^{-1}), microzooplankton (x10^3 cell L^{-}

992 ^{1}), and mesozooplankton (x10^3 ind m^{-3}) abundance collected in the Thau lagoon during the

993 study period. All values represent monthly mean ± SD. In June 2017 (*), the mean (± SD) of

994 mesozooplankton abundance was 90,895 ± 107,072 ind m^{-3}.

995

996

997

998

999

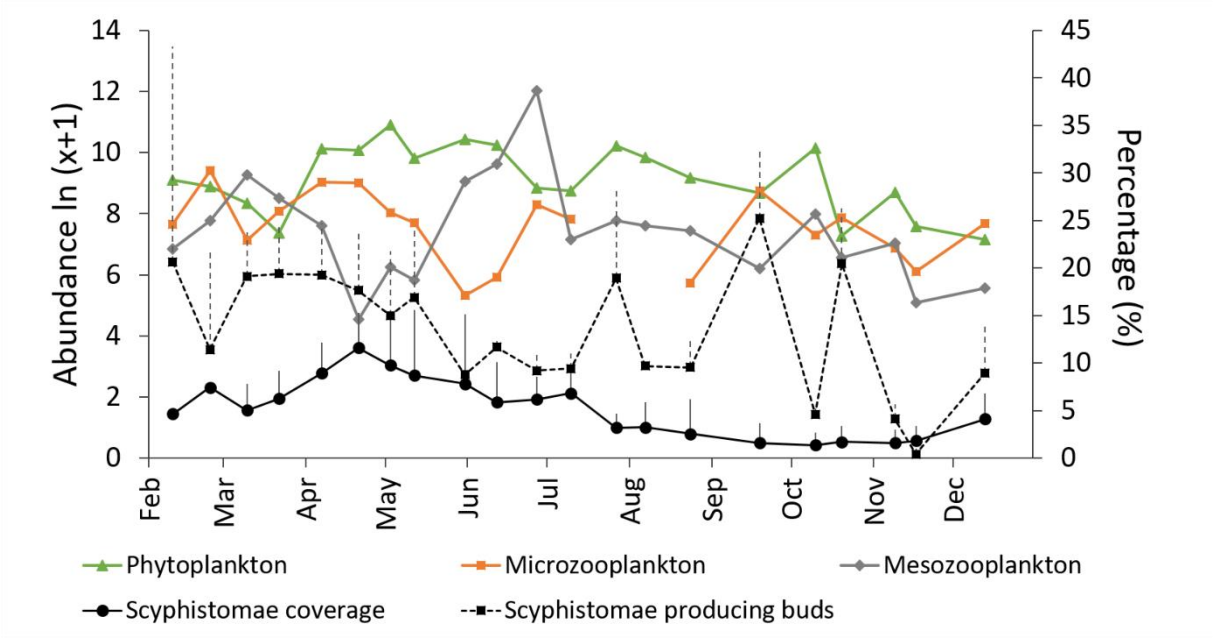

Fig. 4: Temporal variability of the *A. coerulea* benthic population dynamics and the abundance of plankton in the Thau lagoon during the study period (adapted from Marques et al. 2019). Black lines represent the percentage of scyphistomae coverage (i.e., an indicator of population size) and the percentage of the scyphistomae producing buds. Each point represents replicate means and vertical lines are SD (see Marques et al 2019 for further information). Coloured lines represent the non-averaged abundance (after logarithmic transformation) of phytoplankton (cell L^{-1}), microzooplankton (cell L^{-1}), and mesozooplankton (ind m^{-3}).

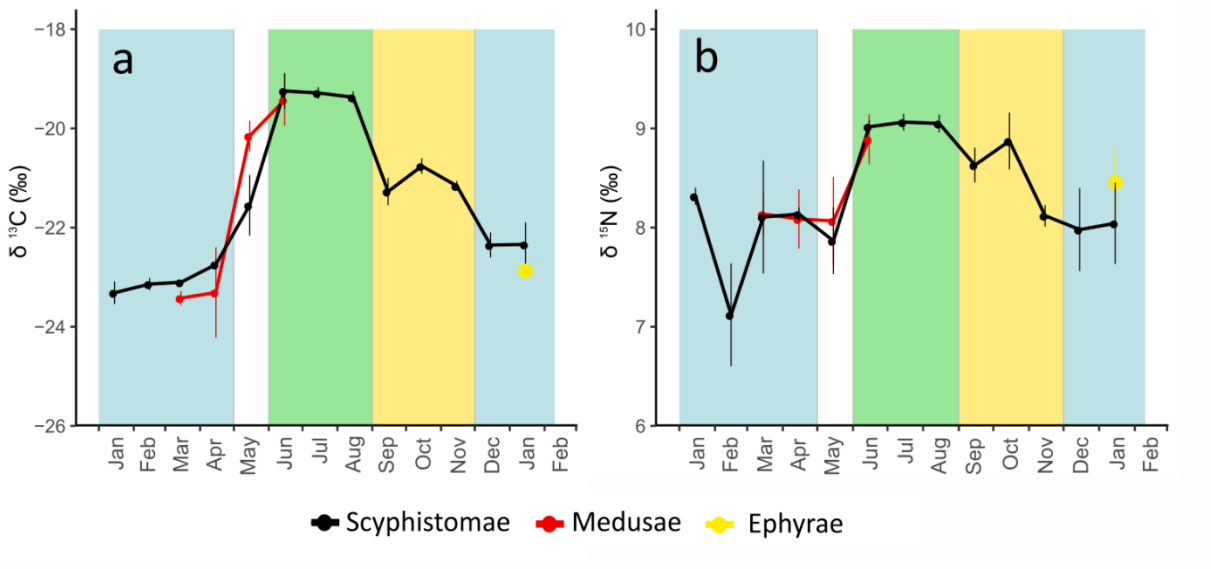

Fig. 5: Temporal variability of $\delta^{13}C$ (a) and $\delta^{15}N$ (b) of *A. coerulea* scyphistomae, medusae, and ephyrae in Thau. All values represent monthly means ± SD. Background colours represent the different isotopic niche periods (periods 1, 2, and 3 in blue, green, and yellow, respectively; see Fig.6). May represents a transitional period and it was not included in any isotopic niche period.

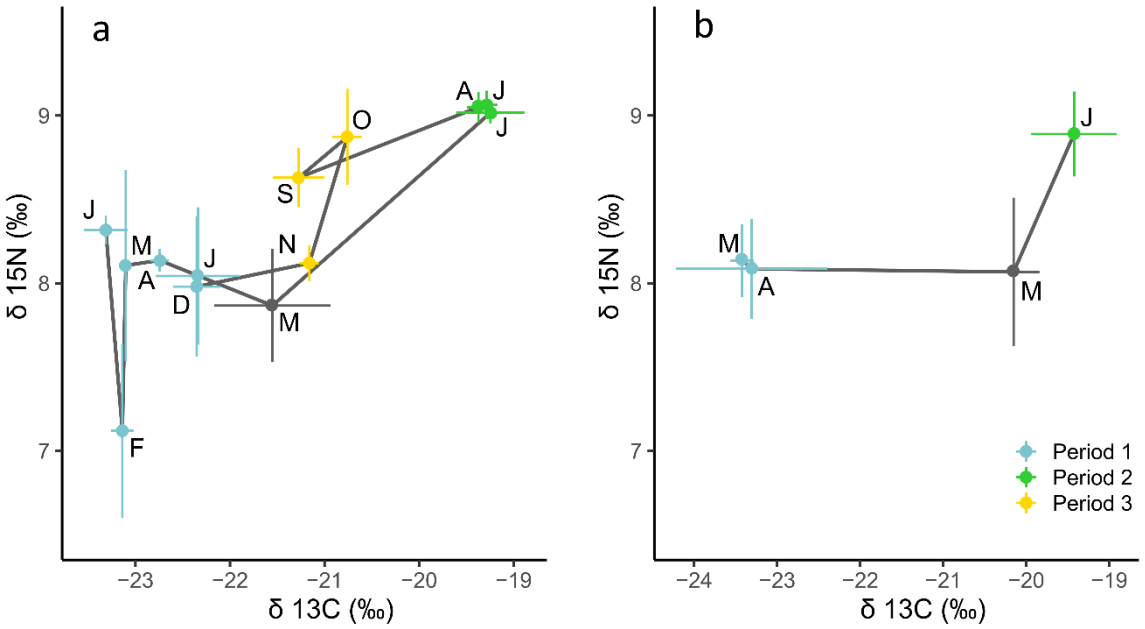

1022

1023 Fig. 6: Time trajectory of the evolution of the isotope signature, averaged by month, from *A.*

1024 *coerulea* scyphistomae (a) and medusae (b). Letters represent months (from January 2017 to

1025 January 2018). Coloured points represent isotopic niche periods defined after cluster analysis:

1026 period 1 is from January to April 2017 and from December 2017 to January 2018; period 2 is

1027 from June to August 2017 and period 3 is from September to November 2017. May represents

1028 the transition between periods 1 and 2 and was therefore not included in any isotopic niche

1029 period.

1030

1031

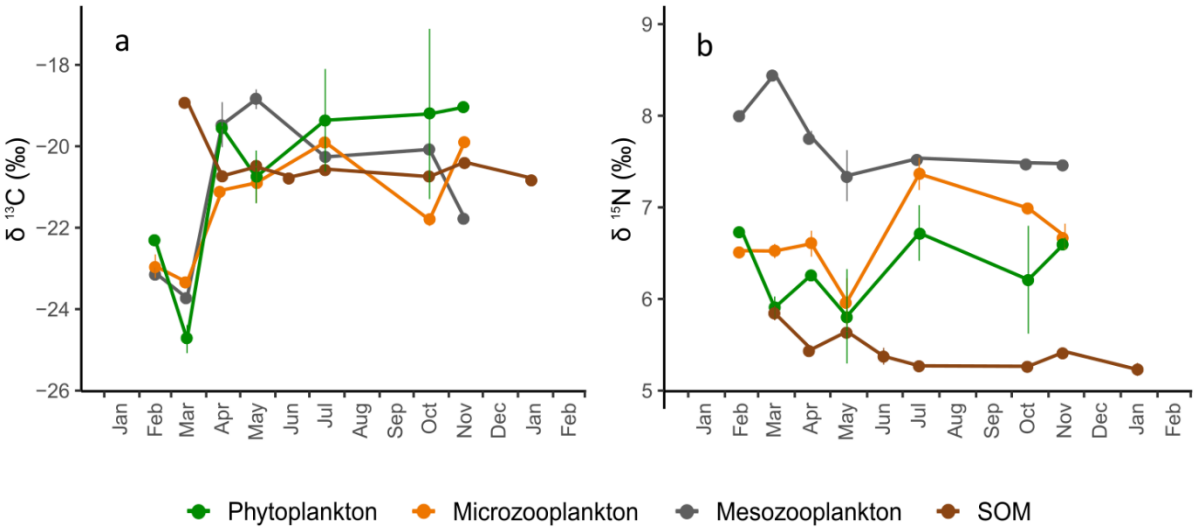

1032

1033 Fig. 7: Monthly variability of the $\delta^{13}C$ (a) and $\delta^{15}N$ (b) of the organic matter sources collected

1034 in this study. SOM: sedimentary organic matter.

1035

1036

1037

1038

1039

1040

1041

1042

1043

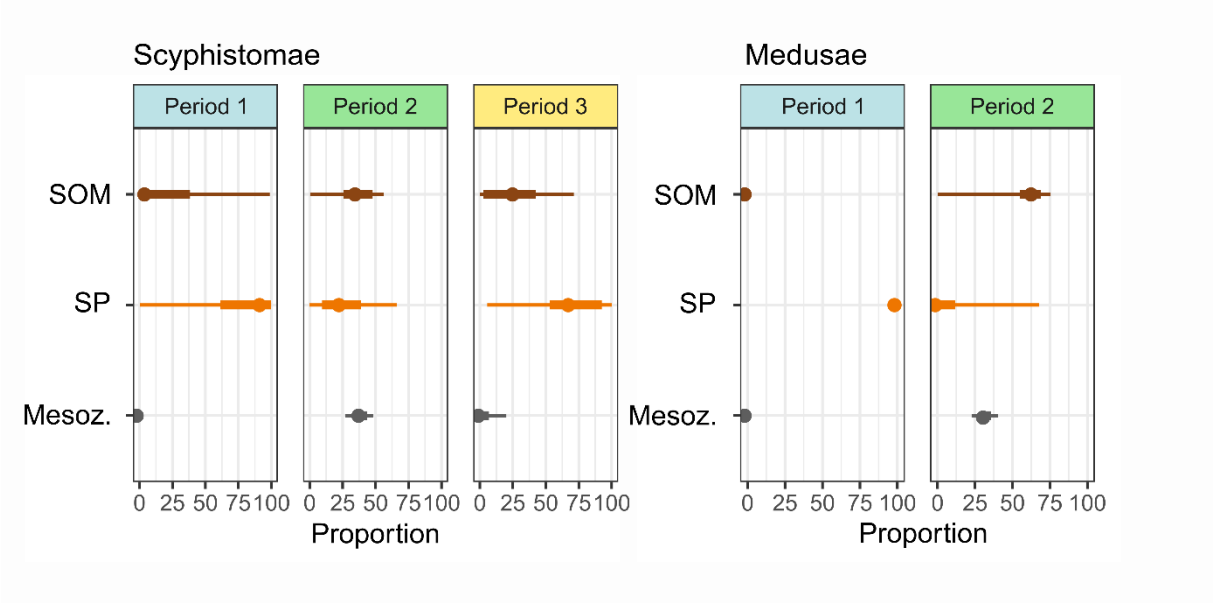

1044

1045 Fig. 8: Proportion of the contribution of each organic matter source to the diet of *A. coerulea*
1046 scyphistomae and medusae during the different isotopic niche periods. The proportion was
1047 calculated using MixSIAR mixing models. The points indicate the median and the horizontal
1048 bars represent 75% and 95% Bayesian credibility intervals. SOM: sedimentary organic matter,
1049 SP: small plankton, Mesoz.: mesozooplankton.

1050

1051

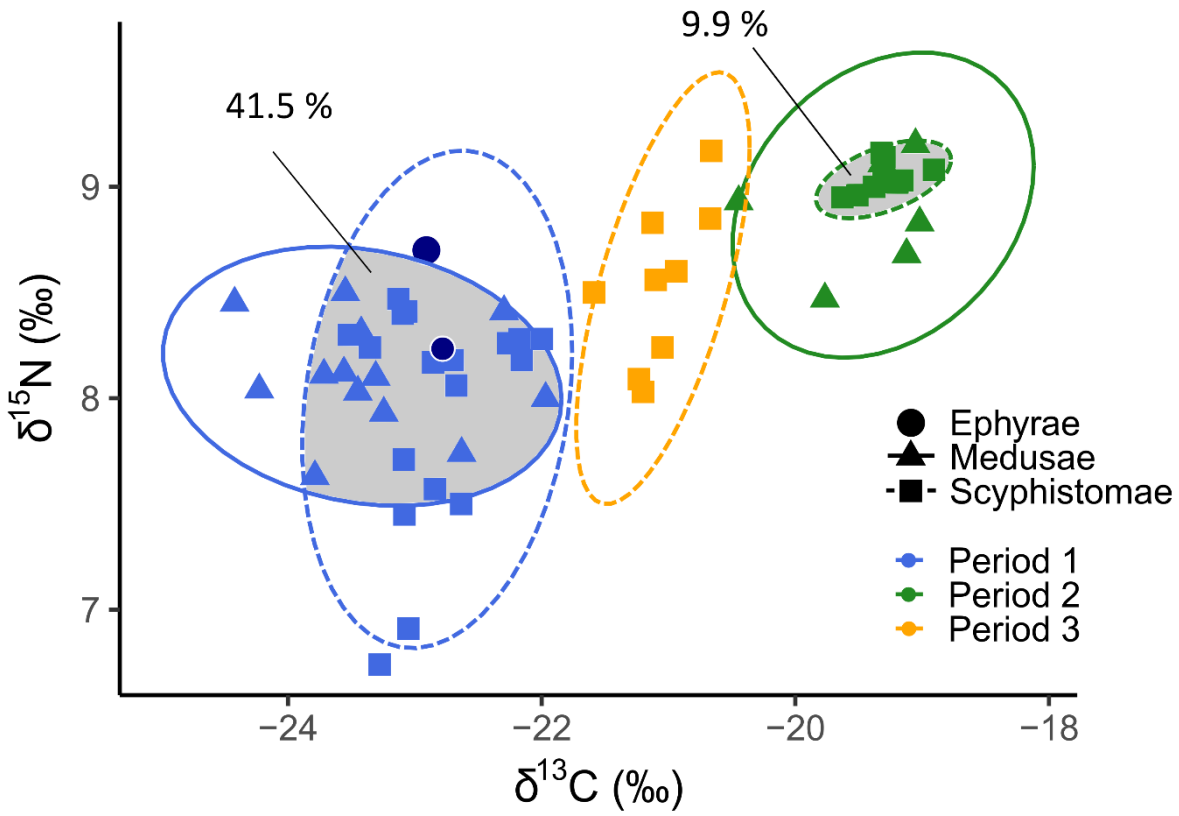

1052

1053 Fig. 9: Biplot of isotope values of *A. coerulea* ephyrae, medusae, and scyphistomae. Ellipses
1054 indicate their isotopic niche in the Thau lagoon (as 95% confidence ellipse of the bivariate
1055 means), during the different isotopic niche periods. Grey areas and associated values indicate
1056 the percentage of overlap, when observed.

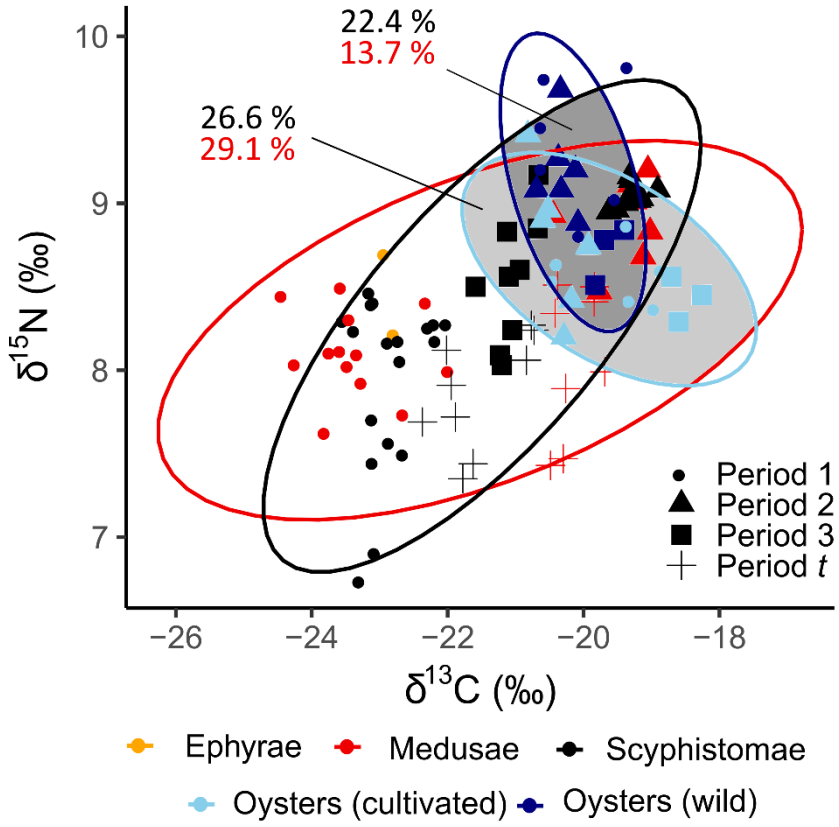

1057

1058 Fig. 10: Biplot of isotope values of *A. coerulea* ephyrae, medusae, scyphistomae, and oysters

1059 (*C. gigas*). Ellipses indicate their isotopic niche in the Thau lagoon, considering the whole

1060 study period (as 95% confidence ellipse of the bivariate means). Dark and light grey areas

1061 indicate niche overlap between *A. coerulea* and wild or cultivated oysters, respectively.

1062 Associated values on the graph indicate the percentage of overlap with medusae (in red) and

1063 scyphistomae (in black). The shape of points represents isotopic niche periods (period *t*:

1064 transitional period, i.e., samples collected in May).

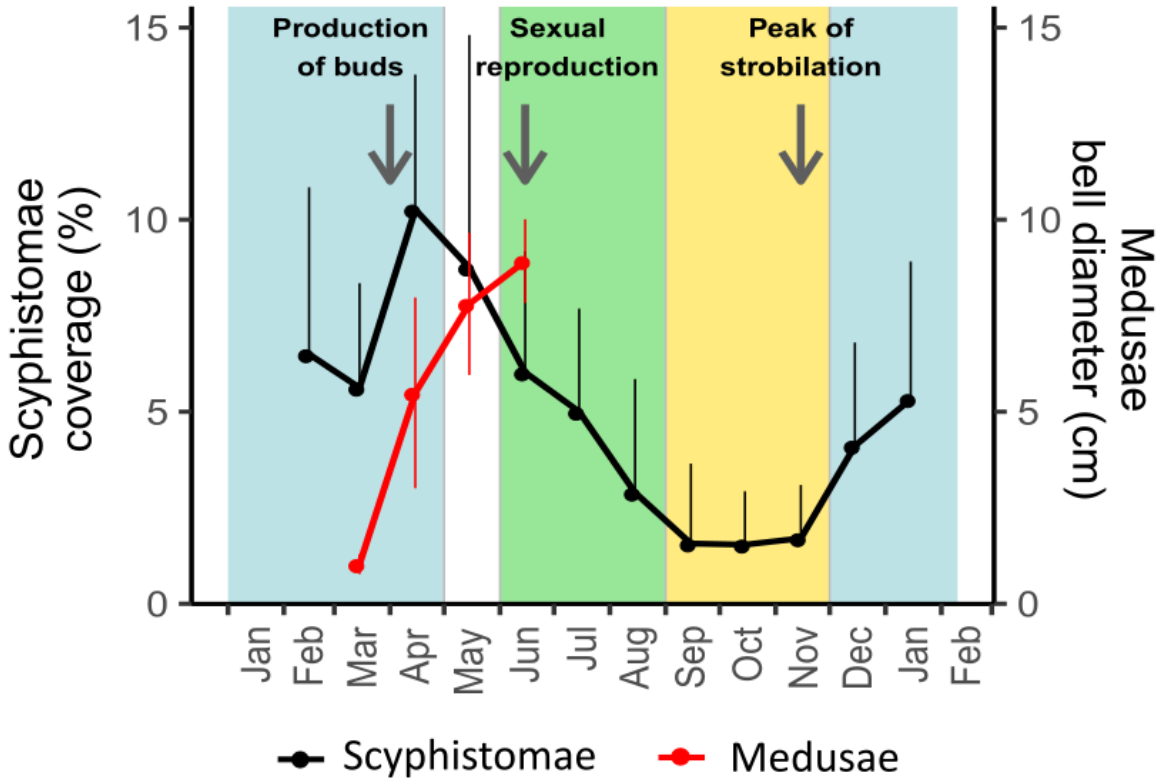

1065

1066 Fig. 6: Scyphistomae coverage (in black, from Marques et al. 2019) and medusae bell

1067 diameter of the individuals collected for stable isotope analysis in this study (in red). The

1068 arrows indicate the main periods of sexual and asexual reproduction of *A. coerulea* (after

1069 Marques et al. 2015b, 2019). The background colours represent the isotopic niche periods

1070 (periods 1, 2, and 3 in blue, green, and yellow, respectively).

1071